Marine and Petroleum Geology 43 (2013) 102–120

Contents lists available at SciVerse ScienceDirect

Marine and Petroleum Geology

journal homepage: www.elsevier.com/locate/marpetgeo

Conceptual modeling of onshore hydrocarbon seep occurrence in the Dezful Embayment, SW Iran

Sanaz Salati [a,b,*], Frank J.A. van Ruitenbeek [a], Emmanuel John M. Carranza [a,1], Freek D. van der Meer [a], Majid H. Tangestani [b]

[a] Faculty of Geo-information Science and Earth Observation (ITC), University of Twente, P.O. Box 6, 7500 AA Enschede, The Netherlands
[b] Department of Earth Sciences, Faculty of Sciences, Shiraz University, 71454 Shiraz, Iran

ARTICLE INFO

Article history:
Received 17 April 2012
Received in revised form
20 February 2013
Accepted 4 March 2013
Available online 14 March 2013

Keywords:
Onshore hydrocarbon seeps
Spatial pattern
Spatial analysis
Conceptual model

ABSTRACT

Petroleum and gas seeps on the ground surface are direct indicators of accumulations of hydrocarbons in the subsurface and could reflect the migration of hydrocarbons in a sedimentary basin. Quantitative analyses of the spatial pattern of hydrocarbon seeps and their spatial associations with geological features could aid in deducing geological controls on their occurrence. In this study the Fry analysis was applied to study the spatial pattern of mapped hydrocarbon seeps, whereas spatial association analyses were implemented to quantify the spatial association of mapped seeps and their alteration products with geological features. The spatial pattern analysis of hydrocarbon seeps showed that oil seeps followed prominent NW–SE and NE–SW trends while gas seeps followed NW–SE and N–S trends suggesting that NNE–SSW and NW–SE fractures are possible migration pathways for hydrocarbons to reach the surface. The results of the spatial association analysis illustrated strong positive spatial associations of oil and gas seeps with the Gachsaran and the Mishan formations, implying upward migration of hydrocarbons through permeable micro-fractures and micro-pores in their strata. A conceptual model has proposed for the occurrence of onshore hydrocarbon seeps in the Dezful Embayment.

1. Introduction

Petroleum and gas seeps on the ground surface are direct indicators of accumulations of hydrocarbons in the subsurface and could reflect the migration of hydrocarbons in a sedimentary basin. Due to high pressures at depths, hydrocarbons in the subsurface can escape to the surface through fractures in rocks and planes of weakness between geological layers.

There are extensive studies about spatial patterns of hydrocarbon seeps in offshore areas (De Boever et al., 2009; Huang et al., 2009; Jin et al., 2011; Washburn et al., 2005) and various conceptual models of hydrocarbon migration in such areas have been proposed (Ding et al., 2008; Leifer and Boles, 2005, 2006). In contrast, few studies have been published about the geological context of hydrocarbon seeps in onshore areas (Clarke and Cleverly, 1991; Link, 1952; MacGregor, 1993). Hydrocarbon seeps are spatially associated with structures such as faults, fractures, folds, unconformities, and salt domes. They can be found within the reservoirs and cap rock formations exposed at the surface. Spatial associations of hydrocarbon seeps with geological features could aid in investigation of cap rock capacity at regional scales (O'Brien et al., 2005; Pinet et al., 2008). In addition, recognition of spatial associations between hydrocarbon seeps with geological features could provide additional valuable information for exploration and environmental programs (Ellis et al., 2001; Etiope et al., 2006).

Methods for quantitative analyses of the spatial pattern of mineral deposits and their spatial associations with geological features have been extensively applied for mineral prospectivity mapping (Carranza, 2009a, b; Carranza and Sadeghi, 2010). Such methods have not yet been applied, however, to study hydrocarbon seep occurrences. Like in mineral prospectivity analysis, quantitative analyses of the spatial pattern of hydrocarbon seeps and their spatial associations with geological features such as faults, fractures, and lithologies could aid in deducing geological controls on their occurrence. Analysis of the spatial pattern of mapped hydrocarbon seeps could provide insights into which geological features control their localization at the surface. In addition, analysis of spatial association of mapped seeps with geological features is instructive in weighing the importance of each geological feature as

* Corresponding author. Faculty of Geo-information Science and Earth Observation (ITC), University of Twente, P.O. Box 6, 7500 AA Enschede, The Netherlands. Tel.: +31 53 4874227; fax: +31 53 4874336.
E-mail addresses: salati@itc.nl, sanaz.salati@yahoo.com (S. Salati).
[1] Present address: School of Earth and Environmental Sciences, James Cook University, Townsville, Queensland 4811, Australia.

0264-8172/$ – see front matter © 2013 Elsevier Ltd. All rights reserved.
http://dx.doi.org/10.1016/j.marpetgeo.2013.03.001

controls on the occurrence of hydrocarbon seeps. Consequently, such analyses would allow development of a conceptual model of how hydrocarbon seeps are localized at the surface and why they occur only at specific sites.

In this paper, we describe quantitatively the spatial pattern of mapped hydrocarbon seeps in the Dezful Embayment, SW Iran. The prime objectives of this study are to obtain insights about (a) links between geological structures such as faults, fold axes and fractures and hydrocarbon seeps and (b) the probability of spatial association of different geological features such as lithological units and their associated structures with oil and gas seeps. We chose the Dezful Embayment for this study because sufficient knowledge exists about the distribution of petroleum at the surface and in the subsurface.

2. Geological setting of the study area

The study area is located in the Zagros fold-thrust belt, SW Iran. The co-existence of rich source rocks, excellent reservoirs, efficient seal, large anticlines and rock fractures resulting from the Zagros folding explain the importance of the Zagros fold-thrust belt as a prolific petroleum province (Bordenave and Hegre, 2005). At least 40–50% of Iranian seeps in the SEEPS database, which was produced by the British Petroleum and described by Clarke and Cleverly (1991), can be linked to underlying hydrocarbon accumulations (MacGregor, 1993).

2.1. General geology

The Zagros fold-thrust belt resulted from the continental collision between the Arabian plate and Iranian block (Berberian and King, 1981). This compressive movement began during Late Cretaceous and became widespread following the continent–continent collision in Miocene, which is still active in N–S direction (Falcon, 1974; Sella et al., 2002; Stocklin, 1968). The convergence direction is oblique to NW–SE trend of the orogenic belt. The Zagros fold-thrust belt, which lies south of the Zagros Suture (Fig. 1), is divided into NW-SE trending structural zones (imbricated and simply folded belt) and laterally divided to Lurestan, Dezful embayment and Fars region (Berberian and King, 1981; Carruba et al., 2006; Falcon, 1974; Motiei, 1993; Sherkati and Letouzey, 2004; Stocklin, 1968).

The Dezful Embayment, situated in the central-southern part of the Zagros fold-thrust belt (Fig. 1), hosts most of the onshore hydrocarbon reservoirs of Iran. This area, which is situated southwest of the Mountain Front Fault (MFF), is dominated by NW–SE trending folds and thrusts. The NW boundary of the Dezful Embayment coincides with the Balarud fault zone (BFZ) and its SE

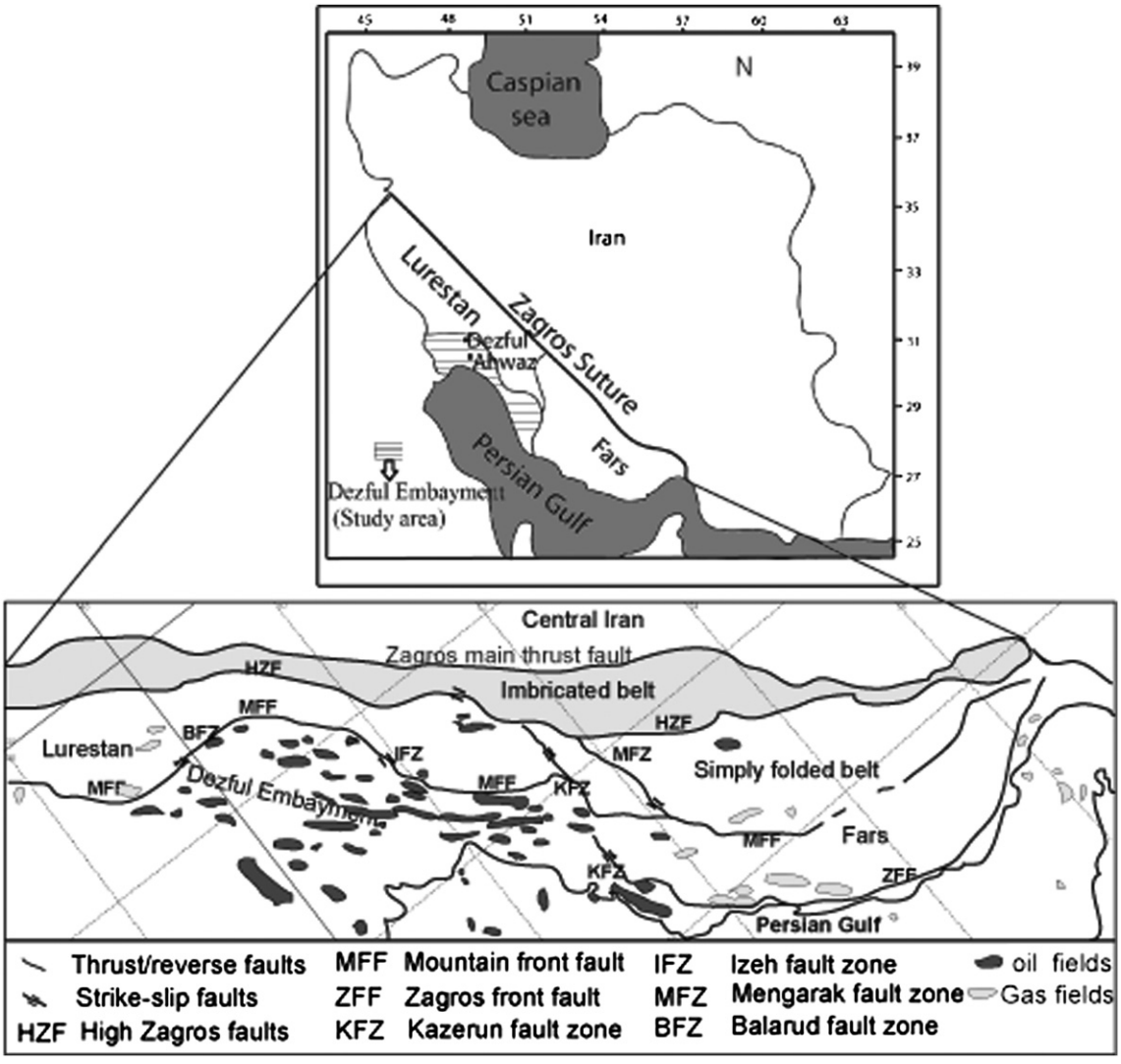

Figure 1. Structural setting of the Zagros fold including locations of oil and gas fields.

boundary is defined by the Kazerun fault zone (KFZ). The NE–SW-trending BFZ, the N–S-trending KFZ and Izeh fault zone (IFZ), and the NW–SE-trending MFF are seismically active (Berberian, 1995) and have significant influence on hydrocarbon entrapment in the Zagros fold-thrust belt (Beydoun et al., 1992; Bordenave and Hegre, 2005; Hessami et al., 2001; McQuillan, 1991).

The stratigraphy of the study area (Fig. 2) is defined by a competent group formed by a structural unit between the lower detachment or lower mobile group (the Hormuz salt) and the upper detachment or upper mobile group (the Gachsaran evaporites) (O'Berian, 1957). The mobile Gachsaran Formation migrated from the crest of anticlines downward and accumulated within synclines, accentuating the asymmetry of the whole structure (Sherkati et al., 2005). This deformation caused severe disharmony between surface structures and the underlying structures (Abdollahi Fard et al., 2011; Alavi, 2004; Bahroudi and Koyi, 2004; Gill and Ala, 1972; Kashfi, 1980; Motiei, 1993; O'Berian, 1957; Sherkati and Letouzey, 2004; Sherkati et al., 2005). The ongoing late Tertiary folding concurrent with deposition, means that the lower member of the Gachsaran Formation (seal) thin as they overlap and wedge out onto growth folds in the Asmari reservoir (Alavi, 2004; Warren, 2006). The base of the Gachsaran Formation forms a major décollement, which shows the repetition by faulting. Several thrusts produced by slip on the basal Gachsaran displace the Gachsaran evaporites and its overlying units (Alavi, 2004).

2.2. Petroleum geology

The Cretaceous to Early Miocene shallow petroleum system of the Dezful Embayment is one of the world richest oil fields because it contains about 8% of global oil reserves (Bordenave and Hegre, 2010). This petroleum system comprises two source rocks including the Kazhdumi and the Pabdeh Formations, two reservoirs including the Asmari and the Sarvak Formation, and two seals including the Gachsaran and the Gurpi Formations.

The Albian Kazhdumi Formation (Kz) consists of bituminous shale with argillaceous limestone. Except in oil fields to the NE of the Dezful Embayment, most of the oil accumulated in the Asmari/Sarvak reservoirs originated from the Kz (Bordenave and Hegre, 2010). The Eocene Pabdeh Formation (Pd) is composed of marls, shales, and carbonates, all rich in pelagic micro-fauna. Recent studies showed that most parts of the Pd, including its limestone beds, were deposited in a ramp environment. The Pd separates the structural traps of the Cretaceous Bangestan Group from the overlying Asmari Formation (Bordenave and Hegre, 2010).

The Asmari Formation contains 75% of the onshore hydrocarbon reserves. Fractures resulting from the Zagros folding enhanced the quality of this limestone reservoir by facilitating the expulsion of oil from source rocks in anticline areas (Bordenave and Hegre, 2005). The Sarvak Formation, which is the second major reservoir, accounts for 23% of hydrocarbon reserves in the Dezful embayment. The Sarvak limestone Formation is often interconnected to the Asmari Formation in high-relief often thrust anticlines and have the same oil water level because of the fracturing of the Pabdeh-Gurpi marls in the crestal part of the anticlines (Bordenave and Hegre, 2005). The Asmari reservoir is sealed by the Gachsaran evaporites. The Gachsaran Formation exhibits rhythmic bedding consisting of bluish-green marl, limestone, dolomite and anhydrite, with/without bedded salt (Gill and Ala, 1972; Motiei, 1993). The Sarvak reservoir is sealed by the Gurpi Formation, which is dominated by marl and thin interlayers of limestone.

Oil migrated from the source rocks through structures formed during the Zagros folding around 10 Ma ago and continued throughout the Late Miocene and Pliocene. Oil expulsion from the Kz and Pd began between 8 Ma and 3 Ma ago during deposition of the Aghajari Formation (Bordenave and Hegre, 2010). Oil expulsion from the source rocks was also coeval with the formation of the

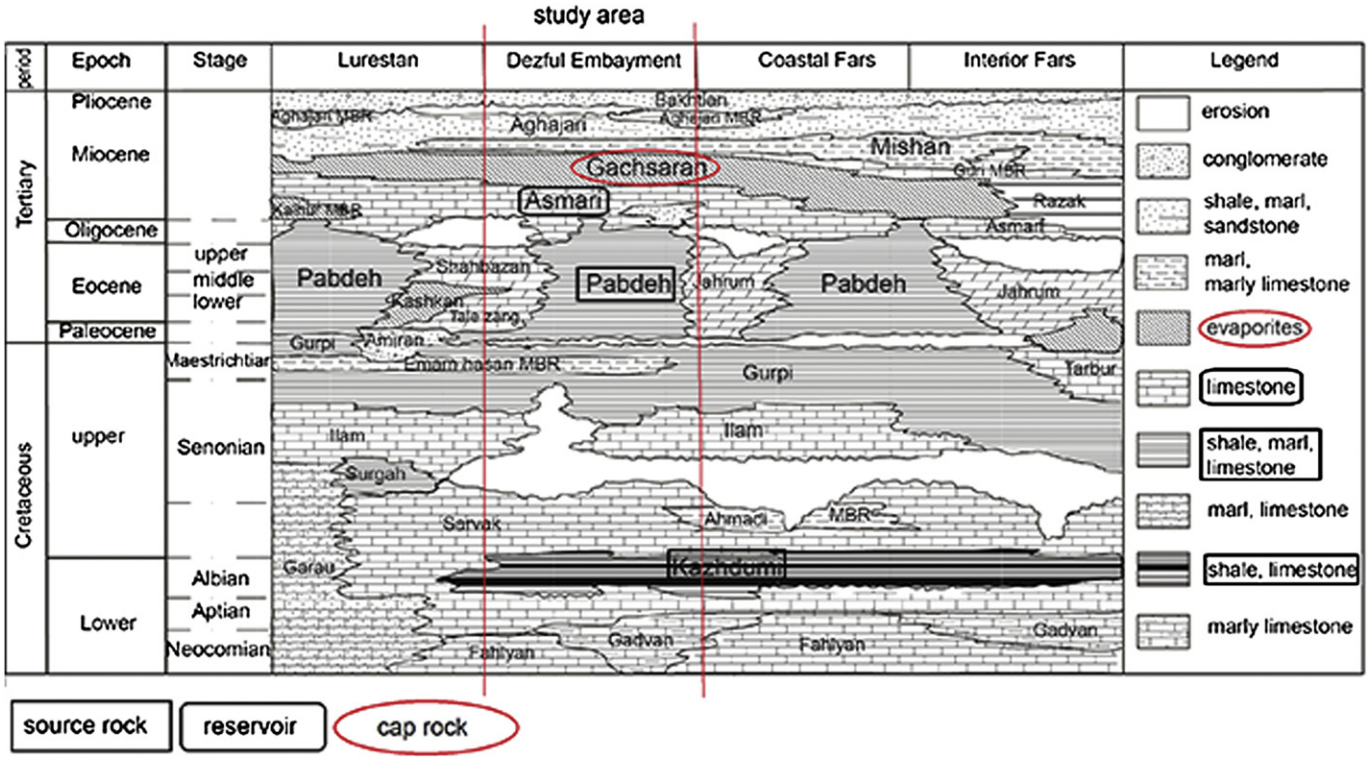

Figure 2. Formations correlation within the Zagros belt (James and Wynd, 1965).

Zagros folds such that hydrocarbons migrated almost vertically to reserves in neighboring anticlines. High pressure in pore spaces of the Kz formed a barrier, however, and prevented oil generated in deeper source rocks from reaching the reservoirs (Bordenave and Hegre, 2010). Oil was expelled from the Pd only in the deeper part of some of synclines, which represent less than 1% of the total oil expelled (Bordenave and Hegre, 2005).

2.3. Hydrocarbon seeps in the Zagros belt

The presence of hydrocarbon seeps led to the discovery of the subsurface petroleum in the SW Iran in early 1900s. There are different types of hydrocarbon seeps in the Zagros fold-thrust belt, such as crude oil, heavy oil or asphalt, gas, gas/oil. Gach-e-tursh and sulphur springs are products of the subsurface alteration processes of gas seeps (Clarke and Cleverly, 1991), which are common in the Dezful Embayment. The term Gach-e-tursh, which was used by Thomas (1952), represents an association of oxidizing petroleum seep, gypsum, jarosite, sulphuric acid, and sulphur.

To the best of the author's knowledge there are few published studies about hydrocarbon seeps in the Zagros oil fields in Iran (Link, 1952; Safari et al., 2011). Based on geological controls, Link (1952) classified seeps into 5 groups. The Zagros hydrocarbon seeps were classified as seeps coming from oil accumulations, which have been eroded or reservoirs ruptured by faulting and folding. By using Remote Sensing techniques, Safari et al. (2011) studied the role of the Kzerun fault on localizing oil and sulfur springs in the Nargesi oil field, SW Iran.

3. Methods

We used 14.1:100,000 scale geological maps of the Dezful Embayment, which have been compiled by the Iranian oil company, to provide lithologic, structural, and hydrocarbon seep maps. Existing knowledge about petroleum systems in the Zagros oil fields (Bordenave, 2002; Bordenave and Hegre, 2010), and extensive studies about the structural framework of the Zagros fold-thrust belt (Berberian, 1995; Bordenave and Hegre, 2005; Carruba et al., 2006; Hessami et al., 2001; McQuillan, 1991; Sepehr and Cosgrove, 2002; Sherkati and Letouzey, 2004) provide us insights into defining geological controls on petroleum systems in the Zagros. Insights into geological controls on hydrocarbon seeps migration and localization can be derived by examining the spatial distribution of hydrocarbon seeps via spatial pattern and spatial association analyses. Because several locations of heavy oil/asphalt seeps and two products of gas seep alteration, namely Gach-e-tursh and sulphur springs, exist in geological maps of the study area, these sub-sets of seeps were used in the spatial analyses.

3.1. Analysis of spatial pattern of hydrocarbon seeps

Hydrocarbon seeps exhibit trends that are similar to trends of faults and anticline axes (Fig. 3) and lithologic units (Fig. 4) in the study area. This illustrates that hydrocarbon seeps in the Zagros oil fields are, in general, structurally controlled (Beydoun et al., 1992; Bordenave and Hegre, 2010; Douglas Elmore and Farrand, 1981; Link, 1952; Rudkiewicz et al., 2007). However, there is a question about which specific sets of geological structures controls the occurrence of each sub-set of hydrocarbon seeps at regional and local scales. An answer to this question can be explored through analysis of the spatial pattern of each sub-set of hydrocarbon seeps. For this purpose, we applied Fry analysis (Fry, 1979) to maps of locations of hydrocarbon seeps in the study area.

Fry analysis is a geometrical method of examining spatial autocorrelation of a set of points, by plotting translations of points whereby each point is used as an origin for translation. Fry analysis describes the spatial pattern of a set of points based on orientations and distances between pairs of translated points. A rose diagram can be created for orientations and frequencies of orientations between all pairs of translated points and pairs of translated points within specific distances. These orientations reveal trends in the points of interest at regional and local scales (Carranza, 2009a,b; Carranza and Sadeghi, 2010). Analysis of point's trends at local scales can be used to deduce processes that localize hydrocarbon occurrences (as points) at certain areas. To analyze trends between any two neighboring seeps, a minimum distance was used within which there is a maximum probability for only one neighbor point next to any one of the points.

We used the DotProc (http://www.kuskov.com) package for Fry analysis. We exported the map coordinates of hydrocarbon seep locations into a delimited file, which is supported by the DotProc software. Fry point coordinates were then exported back into the GIS to visualize and analyze the spatial pattern of seeps. We applied this method to all hydrocarbon seeps and to each sub-set of seeps, as well.

3.2. Analysis of spatial association between hydrocarbon seeps and geological features

Analysis of the spatial association of occurrences of hydrocarbon seeps with geological features could provide insights into which features plausibly controlled those occurrences at specific locations. We applied the distance distribution analysis (Berman, 1977) for quantifying spatial association between hydrocarbon seeps and structural features such as mapped faults and anticline axes. The quantified spatial association refers to the distance or range of distances where hydrocarbon seeps are preferentially located from structural features such as faults and anticline axes. Also, we applied weights-of-evidence (WofE) analysis (Bonham-Carter, 1994) to quantify spatial associations of hydrocarbon seeps with lithologic units.

3.2.1. Distance distribution analysis

The distance distribution analysis quantifies spatial associations between a set of point objects and another set of objects with a particular geometry. It compares a cumulative relative frequency distribution of distances from a set of linear geo-objects to a set of points of interest (denotes as $D(M)$) and a cumulative relative frequency distribution of distances from the same set of linear objects to a set of random point geo-objects (denotes as $D(N)$). In this study, $D(M)$ and $D(N)$ represent, respectively, a cumulative relative frequency distribution of distances from faults and anticline axes to hydrocarbon seeps and a cumulative relative distribution of distances from the same lineaments to a set of random points. The graph of $D(M)$ is compared with the graph of $D(N)$ by computing Kolmogorov–Smirnov statistic to test the null hypothesis that locations of points of interest and linear geo-objects are spatially independent:

$$D = D(M) - D(N) \quad (1)$$

A positive D implies that there is a positive spatial association between the points of interest (hydrocarbon seeps) and the set of linear geo-objects, whereas a negative D implies negative spatial association between them. If $D = 0$, it implies that the locations of points of interest and the linear geo-objects are spatially independent. An upper confidence band for the graph of $D(N)$ curve can be

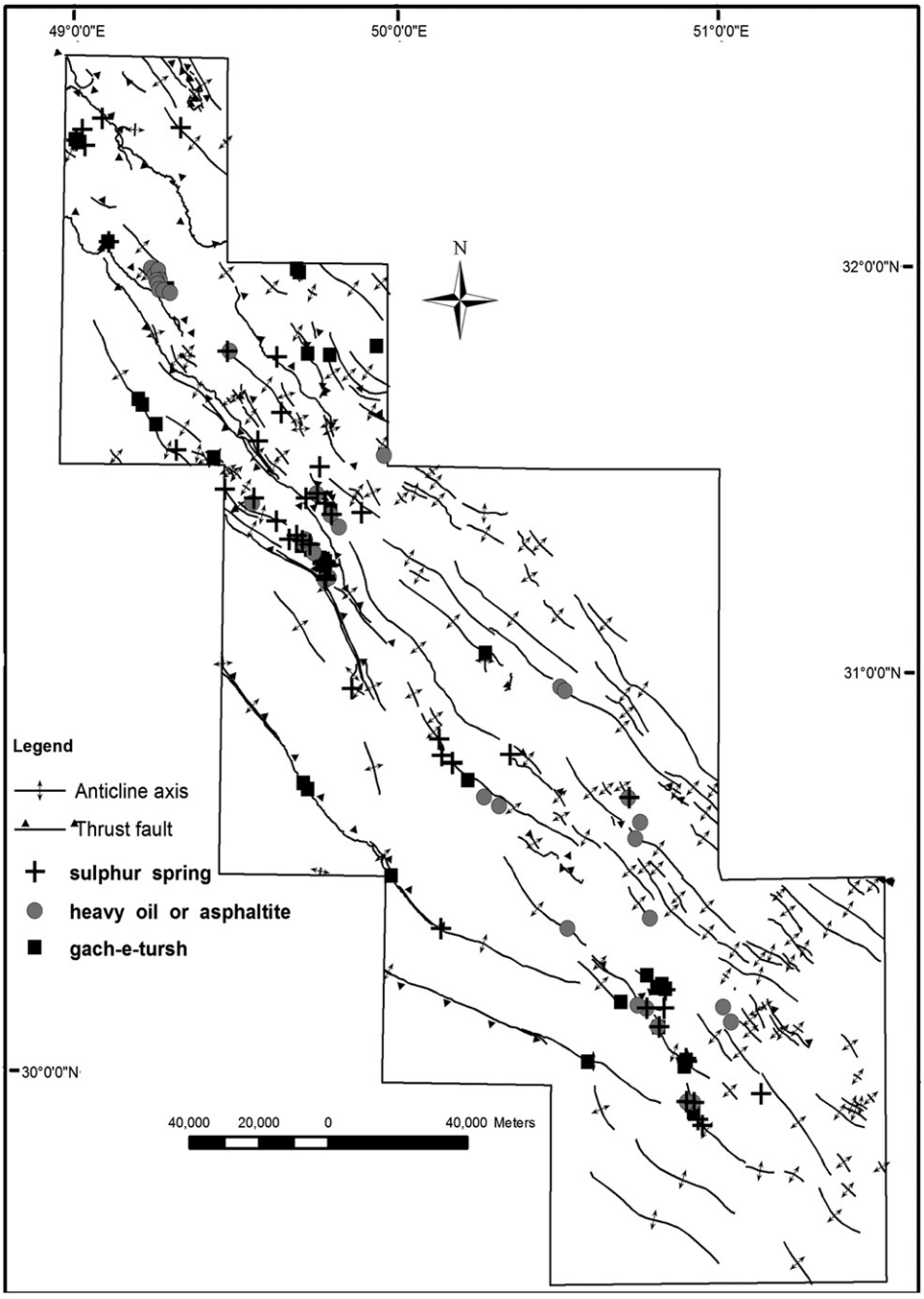

Figure 3. Distribution of faults, anticline axes, and hydrocarbon seeps in the study area.

calculated to determine statistically and graphically if $D(M)$ is greater than $D(N)$ (Berman, 1977):

$$UD(N) = D(N) + \sqrt{9.21\left(\frac{N+M}{4NM}\right)} \quad (2)$$

where M is the number of points of interest and N is the number of random point geo-objects. The value of 9.21 is a critical χ^2 value for 2 degrees of freedom and significance level $\alpha = 0.01$ (Berman, 1977).

The β statistic, which has a χ^2 distribution, can be applied to find the distance from a set of linear geo-objects at which a positive D value is the highest (Berman, 1977):

$$\beta = 4D^2\mathrm{NM}/(N+M) \quad (3)$$

We applied this method to quantifying spatial association of hydrocarbon seeps with faults and anticline axes. The values of D (Eq. (1)) show the spatial association of hydrocarbon seeps with structural features and values of β (Eq. (3)) determine the distance of optimal positive spatial association between the same lineaments and seeps. A positive spatial association ($D > 0$) between a set of hydrocarbon seep locations and a set of geological features suggests that the later represents a set of probable geological controls on the occurrence of the former. The value of β represents an optimal distance from the geological features, which within this distance there is significantly higher proportion of the occurrence of hydrocarbon seeps than would be expected due to chance.

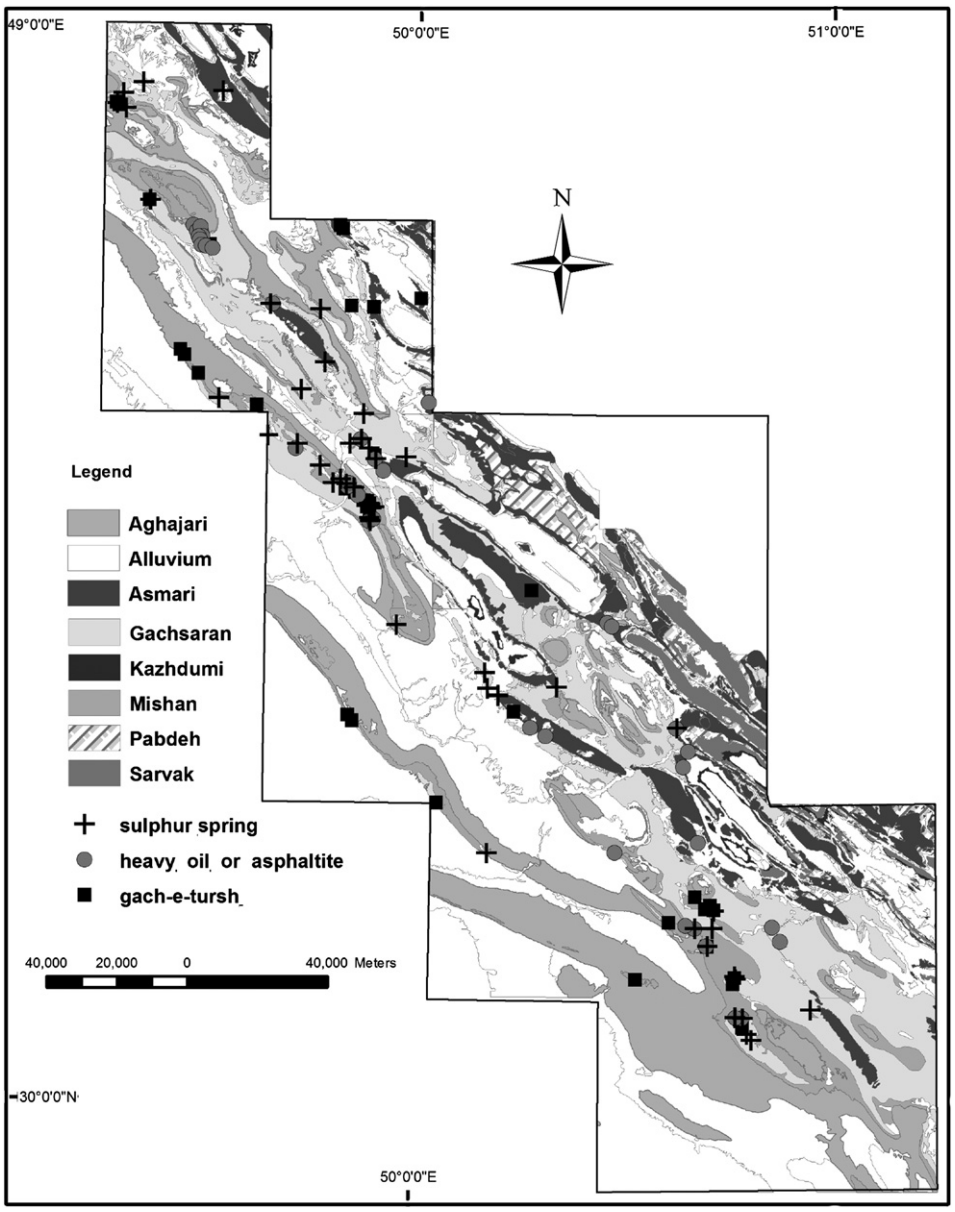

Figure 4. Distribution of hydrocarbon seeps, source rocks (Kazhdumi and Pabdeh Formations), reservoirs (Asmari and Sarvak Formations), cap rock (Gachsaran Formation), and the Mishan Formation.

3.2.2. Weights of evidence (WofE) analysis

The WofE analysis uses a log-linear derivation of Bayesian probability to quantify spatial association between a dependent variable (e.g., hydrocarbon seep occurrence) and an independent variable (e.g., presence of geological features) by statistical means (see (Bonham-Carter, 1994) for more details). In WofE analysis, a positive weight (W^+) and a negative weight (W^-) represent, respectively, positive and negative spatial associations of points of interest D with spatial feature B. The W^+ is calculated as:

$$W^+ = \log_e \frac{P\{B|D\}}{P\{B|\overline{D}\}} \quad (4)$$

and W^- is calculated as:

$$W^- = \log_e \frac{P\{\overline{B}|D\}}{P\{\overline{B}|\overline{D}\}} \quad (5)$$

where B is a binary map of a spatial feature and D is a binary map of points of interest. The $P\{B|D\}/P\{B|\overline{D}\}$ is known as "sufficiency ratio" (LS) and $P\{\overline{B}|D\}/P\{\overline{B}|\overline{D}\}$ is known as "necessity ratio" (LN). These ratios are also known as "likelihood ratios" (Bonham-Carter, 1994). D and B, respectively, indicate the presence of the points of interest and the spatial feature, whereas, $\overline{D}$ and $\overline{B}$, respectively, represent the absence of the points of interest and the spatial feature.

The contrast (C), which is a measure of the spatial association between the points of interest and the spatial features, is calculated as:

$$C = (W^+) - (W^-) \quad (6)$$

We applied the WofE method to provide a measure of spatial association of hydrocarbon seeps (D) with lithologic units (B). A studentized contrast ($SigC$) provides a measure of the certainty with which the contrast is known (Bonham-Carter, 1994). It is defined as the ratio of the contrast divided by its standard deviation. The studentized contrast ($SigC$) is calculated as (Bonham-Carter, 1994):

$$SigC = \frac{C}{\sqrt{s^2(W^+) + s^2(W^-)}} \quad (7)$$

A *SigC* greater than 2 suggests a statistically significant spatial association. The maximum *SigC* is used as index of significant spatial association between hydrocarbon seeps and lithological units.

4. Results

4.1. Spatial patterns of hydrocarbon seeps

Mapped hydrocarbon seeps in the Dezful Embayment show prominent 315°± 15 trend (Fig. 5), which is roughly the same as the general trend of folds and faults in the Zagros fold-thrust belt. Fry plots of hydrocarbon seeps at local scales (<43 km) show subsidiary NNE–SSW trend (Fig. 5a). At the local scale, the Fry plots of heavy oil or asphalt seeps show a prominent NW–SE trend and a subsidiary NNE–SSW trend (Fig. 6). The Fry plots of Gach-e-tursh and sulphur springs show prominent NW–SE and subsidiary N–S trends (Figs. 7a and b). These trends seem correspond with trends of major lineaments that are either perpendicular or parallel to (a) the general trend of the Zagros folds related to the shortening trend of the Zagros (NE–SW) and (b) the trends of basement faults (N–S and NW–SE). These indicate the ongoing influence of NW–SE and NNE–SSW trending faults and/or fractures on the occurrence of hydrocarbon seeps in the Dezful Embayment.

It is known that there is a close correlation between the oil production pattern and structures trending NNE–SSW (McQuillan, 1991) or N–S (Edgell, 1996). Thrust faults exposed to the surface are

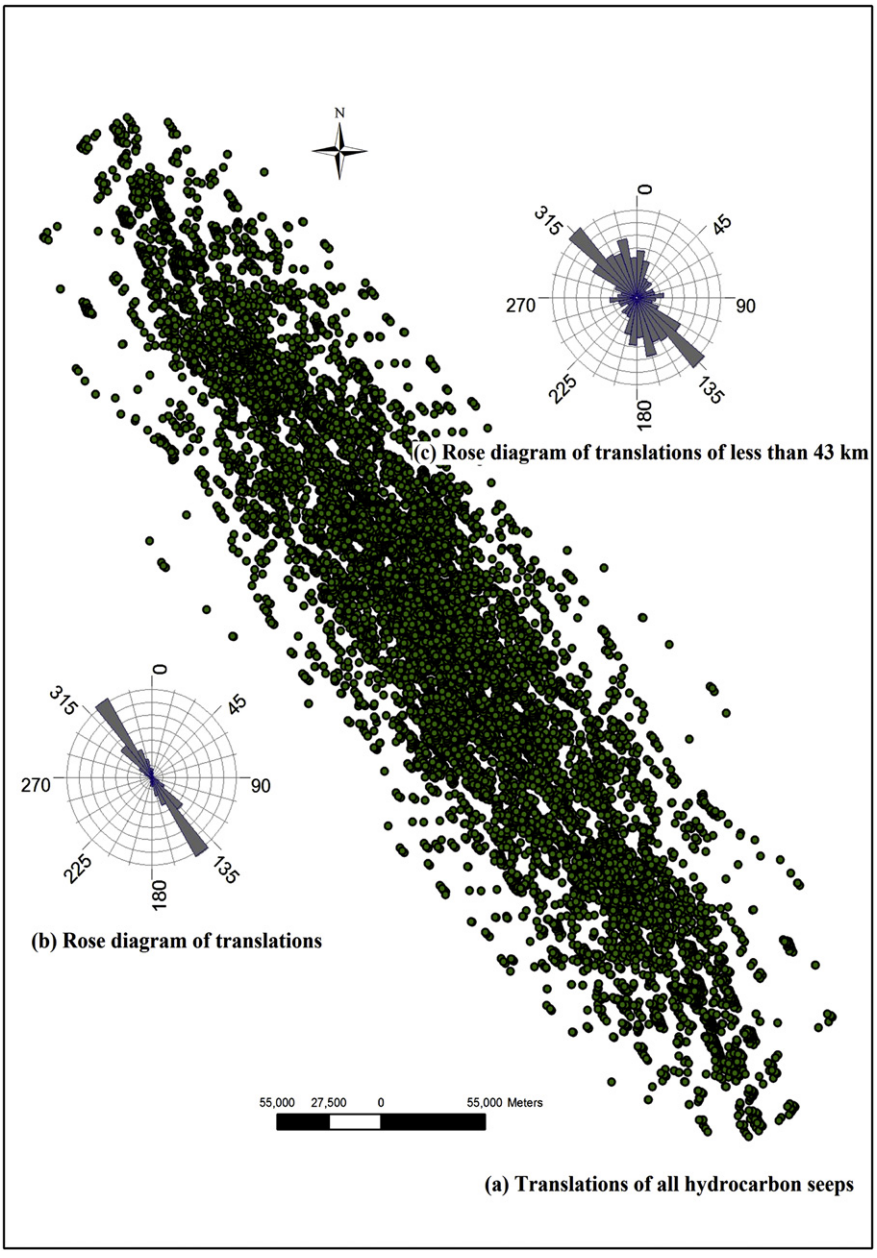

Figure 5. Fry plots and trends of pairs of Fry points of locations mapped hydrocarbon seeps.

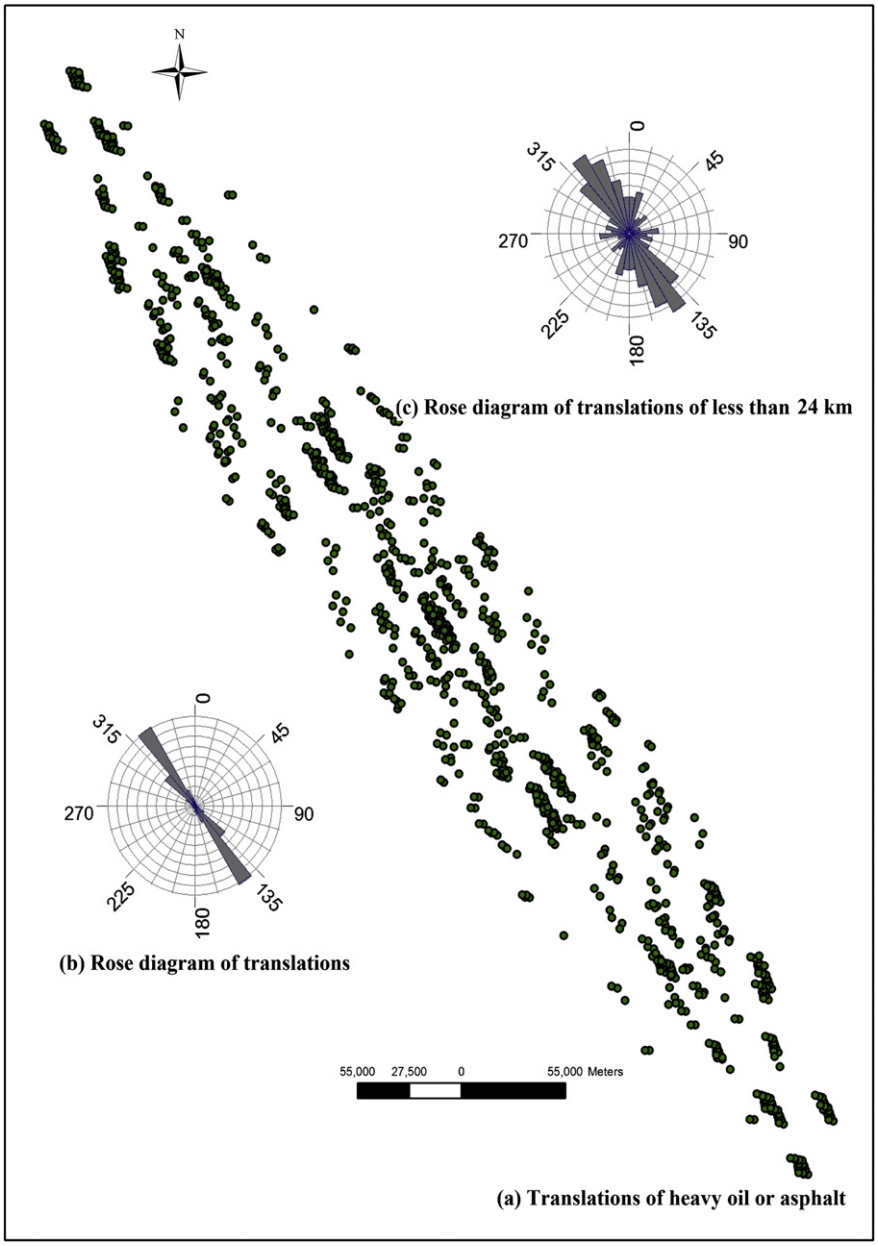

Figure 6. Fry plots and trends of pairs of Fry points of locations mapped heavy oil or asphalt seeps.

parallel to the NW-SE trending folds and are mostly located at the southwestern limb of anticlines. In addition, there are two types of fractures in the Dezful Embayment (Lacombe et al., 2011; Mobasher and Babaie, 2007; Stephenson et al., 2007; Wennberg et al., 2007): fold related fractures and fault related fractures. The 45 ± 5°(NE–SW) trend of all hydrocarbon seeps is perpendicular to the axial trace of anticlines. This trend, which is possibly related to fold- and/or fault-related fractures, is strongly evident in the Fry plots of Gach-e-tursh at the local scale (Fig. 7a). At the local scale, the Fry plots of the Gach-e-tursh and sulphur springs show a prominent 160°–170° (roughly N–S). This trend is plausibly due to fractures formed at small oblique angles to the main N–S (10 ± 5°) trending faults (e.g., Kazerun) (Mobasher and Babaie, 2007). The subsidiary E-W trend (80°–90°) of mapped hydrocarbon seeps is plausibly related to fractures oblique to NW–SE trending folds, NW–SE trending faults, and N–S trending basement faults.

By inference from the analyses of the spatial patterns of mapped hydrocarbon seeps in the study area, it is likely that NNW–SSE trending faults/fractures are plausible structural controls on the occurrences of oil and gas seeps. Heavy oil or asphalt seeps showed the prominent NW–SE trend, which is the same as the general trend of folds. Gas seep alteration products (Gach-e-tursh and sulphur springs) showed the prominent NNW–SSE trends, which are similar to the general trends of folds and basement faults. The results of the spatial pattern analyses can be interpreted further by analysis of spatial associations between mapped seeps and structural and lithological units.

4.2. Spatial associations of hydrocarbon seeps with structural units

Heavy oil or asphalt seeps have positive spatial association with anticlines (Fig. 8a). Within 4 km of anticline axes, 78% of heavy oil

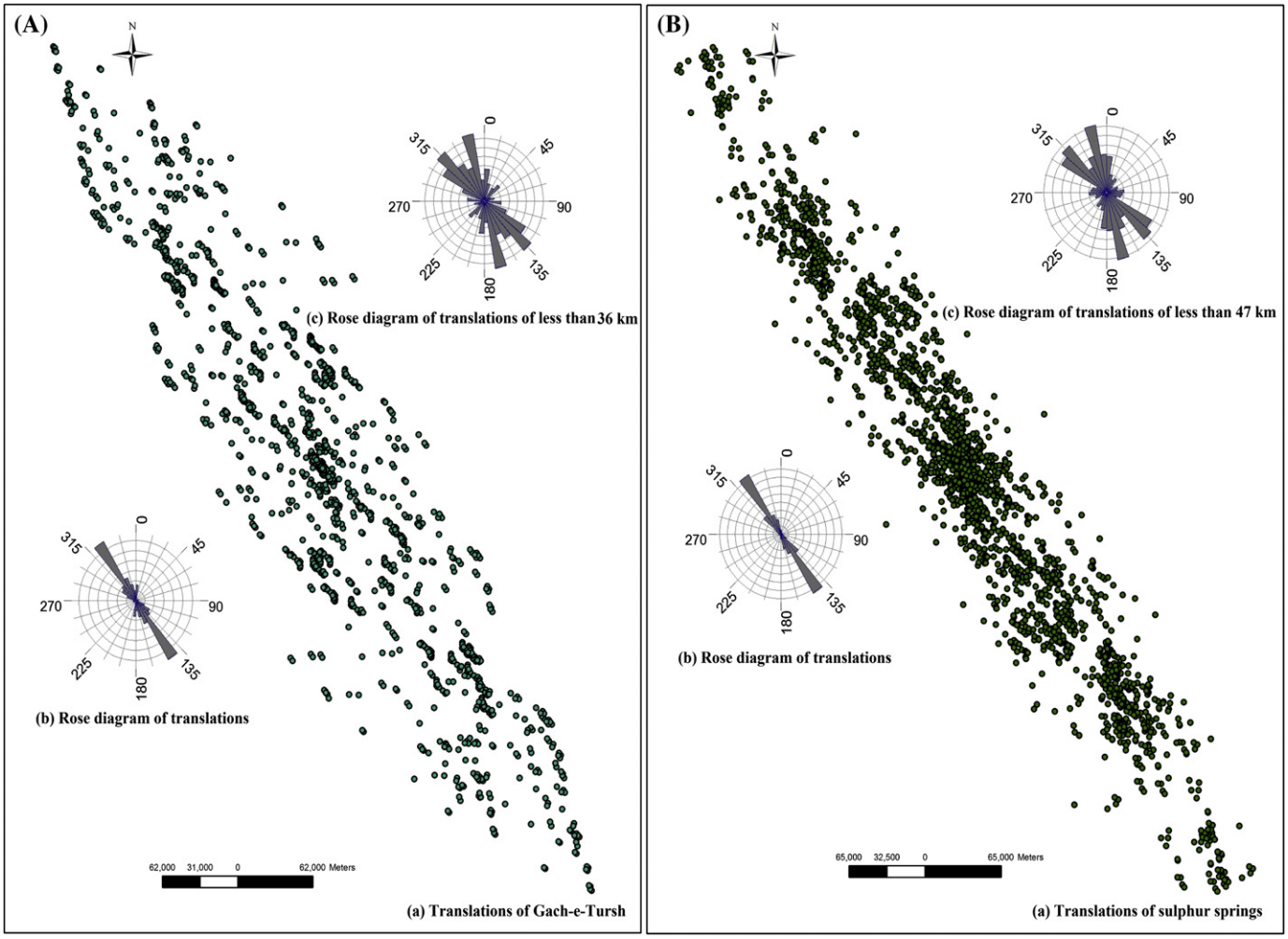

Figure 7. Fry plots and trends of pairs of Fry points of locations mapped (A) Gach-e-Tursh seeps, and (B) sulphur springs.

or asphalt seeps are present. Based on the curve of *D*, there is at most 22% higher occurrence of heavy oil or asphalt seeps than would be expected due to chance (Fig. 8a). As indicated in Figure 8b, there is positive spatial association between heavy oil or asphalt seeps and thrust faults. It appears in Figure 8b that about 60% of the heavy oil or asphalt seep occurrences are within 6 km of the mapped thrust faults suggesting that fault related fractures or/and non-fault related fractures can provide pathways for heavy oil seeps to reach the surface.

Sulphur springs have positive spatial association with anticline axes (Fig. 8c) and thrust faults (Fig. 8d). However, these spatial associations are not statistically significant (at $\alpha = 0.01$). The two peaks in the *D* curve (Figs. 8c) imply that there are two groups of sulphur springs in the area. The first group is comprised of about 30% of the sulphur springs located about an average of 1 km away from anticline axes. The second group is comprised of about 70% of springs located about an average of 4 km away from anticline axes. It appears in Figure 8c that about 78% of the sulphur springs occurrences are within 10 km of the mapped thrust faults.

Gach-e-tursh shows weak but significant (at $\alpha = 0.05$) positive spatial association with anticline axes. As indicated in Figures 8e, 38% of the Gach-e-tursh is located within 1 km of the mapped anticline axes. Within 1 km of anticline axes, there is at most 20% higher frequency of Gach-e-tursh than would be expected due to chance. The Gach-e-tursh shows statistically significant (at $\alpha = 0.01$) positive spatial association with thrust faults (Figs. 8f).

4.3. Spatial association of hydrocarbon seeps with lithological units

Table 1 presents the weights and contrast values calculated for each lithologic unit with respect to the heavy oil or asphalt seeps, Gach-e-tursh, and sulphur springs. The hydrocarbon seeps exhibit positive spatial associations with the Asmari (reservoir), Gachsaran (cap rock), and Mishan Formations.

The Gachsaran Formation shows significant positive spatial association with heavy oil or asphalt seeps. Heavy oil or asphalt seeps have positive spatial associations with the Asmari and Mishan Formations. Heavy oil or asphalt seeps lack spatial associations with the other lithological units with negative values of *SigC*.

Gach-e-tursh and sulphur springs show a significant positive spatial association with the Mishan Formation and positive spatial association with the Gachsaran Formation. The other lithological units do not show spatial associations with sulphur springs and Gach-e-tursh.

The quantified spatial associations of lithological units with mapped hydrocarbon seeps and their alteration products are coherent with facts that the densities of oil and gas seeps are not decreased upwards in the stratigraphy.

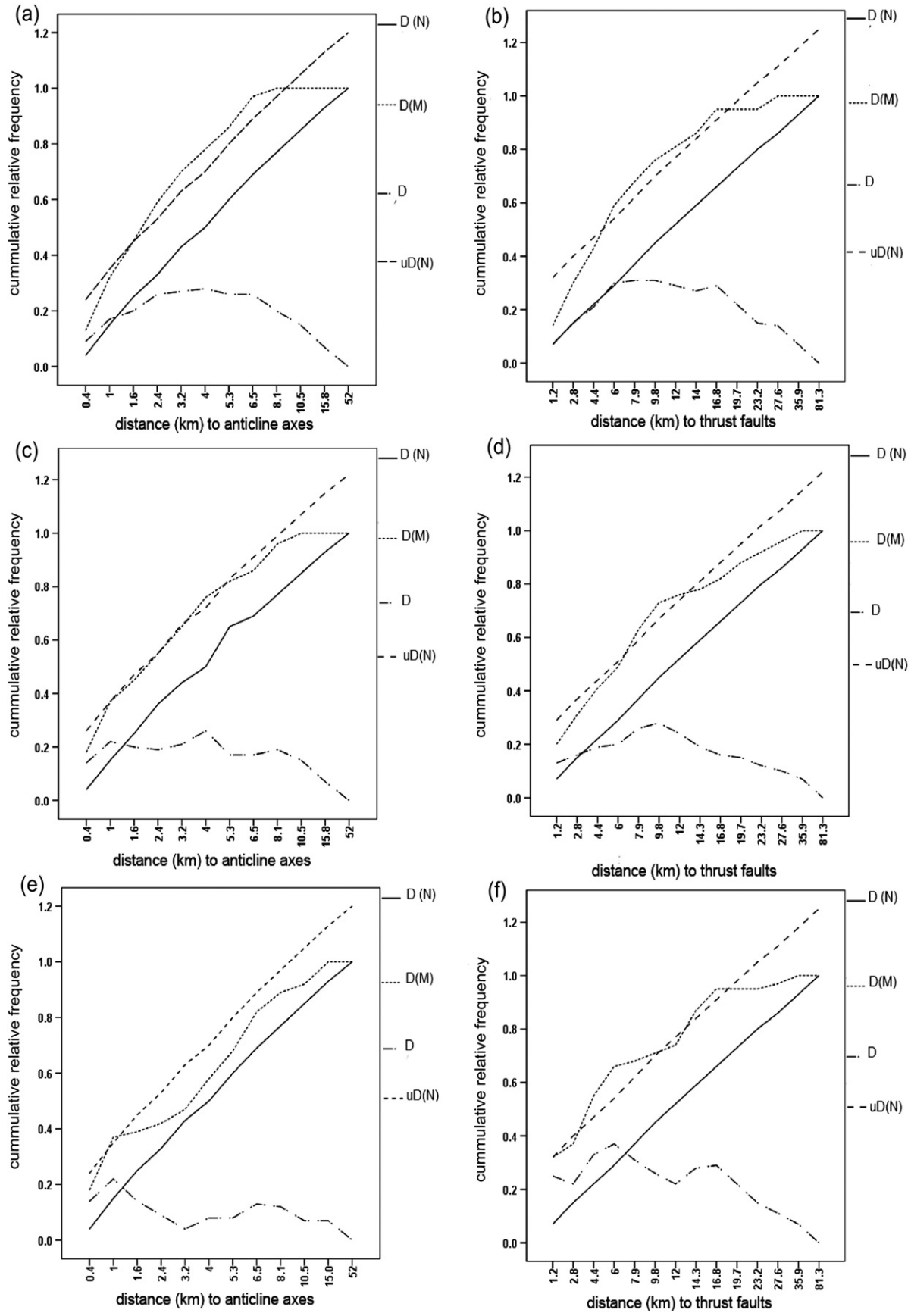

Figure 8. Graphs of cumulative relative frequency of distances at seep locations ($D(M)$) and non-seep locations ($D(N)$) around structural units in the Dezful Embayment. D and u $D(N)$ represent spatial association of seeps with structures and confidence band for $\alpha = 0.01$ respectively. (a) and (b) show analysis of spatial association of heavy oil or asphalt seeps with anticline axis and with thrust faults; (c) and (d) represent analysis of spatial association of sulphur springs with anticline axis and with thrust faults; (e) and (f) show analysis of spatial association of Gach-e-Tursh with anticline axis and with thrust faults.

Table 1
Variation of weights and contrasts for lithologic units with respect to (a) heavy oil or asphalt seeps; (b) Gach-e-tursh; and (c) sulphur springs. Values in bold represent statistically significant positive spatial associations.

Variation of weights and contrasts for lithological units with respect to heavy oil or asphalt seeps

Lithologic units	W^+	W^-	C	$SigC$
Alluvium	0.006	0.14	−0.13	−0.27
Bakhtiari	0	0.076	−0.076	−0.15
Lahbari	0	0.09	−0.09	−0.18
Aghajari	−1.14	0.11	−1.15	−2.3
Mishan	0.8	−0.06	0.86	1.72
Gachsaran	1.3	−0.05	1.63	**3.26**
Asmari	1.09	−0.02	1.11	**2.22**
Gadvan	0	0.001	−0.001	−0.002
Gurpi	0	0.009	−0.009	−0.019
Hurmuz	0	0.0002	−0.0002	−0.0004
Kazhdumi	0	0.003	−0.003	−0.006
Pabdeh	0	0.2	−0.2	−0.4
Sarvak	0	0.02	−0.02	−0.04
Daryan	0	0.0002	−0.0002	−0.0004
Fahlyan	0	0.003	−0.003	−0.006
Shahbazan	0	0.0002	−0.0002	−0.0004
Tutak	0	0.0002	−0.0002	−0.0004

Variation of weights and contrasts for lithologic units with respect to *Gach-e-tursh*

Lithologic units	W^+	W^-	C	$SigC$
Alluvium	−1.06	0.25	−1.31	−1.35
Bakhtiari	0	0.076	−0.076	−0.078
Lahbari	0	0.09	−0.09	−0.092
Aghajari	0	3.11	−3.11	−3.2
Mishan	2	−0.39	2.39	**2.4**
Gachsaran	1.08	−0.45	1.53	1.57
Asmari	−0.28	−0.3	0.3	−0.3
Gadvan	0	0.001	−0.001	−0.001
Gurpi	0	0.009	−0.009	−0.01
Hurmuz	0	−0.0002	−0.0002	−0.0002
Kazhdumi	0	0.003	−0.003	−0.003
Pabdeh	0.59	−0.025	0.615	0.6
Sarvak	0	0.02	−0.02	−0.02
Daryan	0	0.0018	−0.0018	−0.005
Fahlyan	0	0.005	−0.005	−0.005
Shahbazan	0	0.0002	−0.0002	−0.0002
Tutak	0	0.0002	−0.0002	−0.0002

Variation of weights and contrasts for lithologic units with respect to sulphur springs

Lithologic units	W^+	W^-	C	$SigC$
Alluvium	−0.2	0.07	−2.07	−3.45
Bakhtiari	0	0.076	−0.076	−0.13
Lahbari	0	0.09	−0.09	−0.15
Aghajari	0	0.16	−0.16	−0.3
Mishan	1.53	−0.2	1.75	**2.9**
Gachsaran	1.13	−0.5	1.63	**2.7**
Asmari	−1.2	0.05	−1.25	−2.08
Gadvan	0	0.001	−0.001	−0.001
Gurpi	0	0.009	−0.009	−0.01
Hurmuz	0	0.0002	−0.0002	−0.0003
Kazhdumi	0	0.003	−0.003	−0.005
Pabdeh	−0.33	0.008	−0.34	0.6
Sarvak	0.02	0.02	−0.02	−0.03
Daryan	0	0.0018	−0.0018	−0.003
Fahlyan	0	0.003	−0.003	−0.005
Shahbazan	0	0.0002	−0.0002	−0.0003
Tutak	0	0.0002	−0.0002	−0.0003

4.4. Spatial association of sub-sets of hydrocarbon seeps with structures only in lithological units having positive spatial association

The results of the spatial association analysis show that heavy oil or asphalt seeps have significant positive spatial associations with anticline axes in the Asmari reservoir, Gachsaran, and Mishan Formations (Fig. 9a, c and e). These positive spatial associations are optimal within 2.6 km of the anticline axes in the Asmari Formation (Fig. 9b), within 5.8 km of anticline axes in the Gachsaran Formation (Fig. 9d), and within 3.8 km of anticline axes in the Mishan Formation (Fig. 9f). Within 2.6 km, there is 100% occurrence of known heavy oil or asphalt seeps of the anticline axes in the Asmari Formation (Fig. 9a). Within 5.8 km of anticline axes of the Gachsaran Formation, there is at least 50% higher frequency of heavy oil or asphalt seeps than would be expected due to chance (Fig. 9c). According to the curve *D* in Figure 9e, within 3.8 km of the anticline axes in the Mishan Formation, there is at least 85% higher frequency of heavy oil or asphalt seeps than would be expected due to chance. From the curve *D*, it appears that heavy oil or asphalt seeps have stronger positive spatial association with anticline axes in the Asmari Formation. These results are coherent with the fact that oil seeps occurring close to the Oligocene Asmari Formation represent the final exhaustion of former oil accumulations (Douglas Elmore and Farrand, 1981).

Figure 10 shows the analyses of spatial associations of heavy oil or asphalt seeps with thrust faults in the three lithologic formations having positive spatial associations with these seeps. There is no positive spatial association between heavy oil or asphalt seeps within 15 km of thrust faults in the Asmari Formation (Fig. 10a), but this sub-set of seeps have positive spatial associations with thrust faults in the Gachsaran and Mishan Formations (Fig. 10c and e). The two peaks in the *D* and β curves (Fig. 10c and d) imply that there are two groups of heavy oil or asphalt seeps with respect to thrust faults in the Gachsaran Formation. The first group is comprised of about 70% of the heavy oil or asphalt seeps located about an average of 3.8 km away from thrust faults. The second group is comprised of about 30% of heavy oil or asphalt seeps located about an average of 10.4 km away from thrust faults. The positive spatial association of heavy oil or asphalt seeps is optimal within 5.4 km of thrust faults in the Mishan Formation (Fig. 10f).

Figure 11 shows the analyses of spatial association of Gach-e-tursh with structures in the Mishan and Gachsaran Formations. There are statistically significant (at $\alpha = 0.01$) positive spatial associations between Gach-e-tursh and structures in the Gachsaran Formation (Fig. 11a and c). The two peaks in the *D* and β curves (Fig. 11b) imply that there are two groups of Gach-e-tursh with respect to anticline axes in the Gachsaran Formation. The first group is comprised of about 78% of the Gach-e-tursh located about an average of 5.8 km away from anticline axes. The second group is comprised of about 22% of Gach-e-tursh located about an average of 10.9 km away from anticline axes. There are also two peaks in the *D* and β curves of the spatial association of the Gach-e-tursh with thrust faults in the Gachsaran Formation. The first group is comprised of about 85% of the Gach-e-tursh located about an average of 5.4 km away from thrust faults. The second group is comprised of about 15% of Gach-e-tursh located about an average of 10.4 km away from thrust faults.

The Gach-e-tursh has statistically significant (at $\alpha = 0.01$) positive spatial associations with structures in the Mishan Formation (Fig. 11e and g). The positive spatial association is optimal at 6.8 km of the anticline axes (Fig. 11f). The two peaks in the *D* and β curves (Fig. 11g and h) imply that there are two groups of Gach-e-tursh with respect to thrust faults of the Mishan Formation. The first group is comprised of about 63% of the Gach-e-tursh located about an average of 5.4 km away from thrust faults. The second group is comprised of about 37% of Gach-e-tursh located about an average of 15 km away from thrust faults.

Sulphur springs have positive spatial association with anticline axes and thrust faults in the Gachsaran Formation (Fig. 12a and c). Within 2 km of anticline axes and thrust faults in the Gachsaran Formation, there are at least 70% and 50% of known sulphur springs, respectively. The two peaks in the *D* and β curves (Fig. 12c and d)

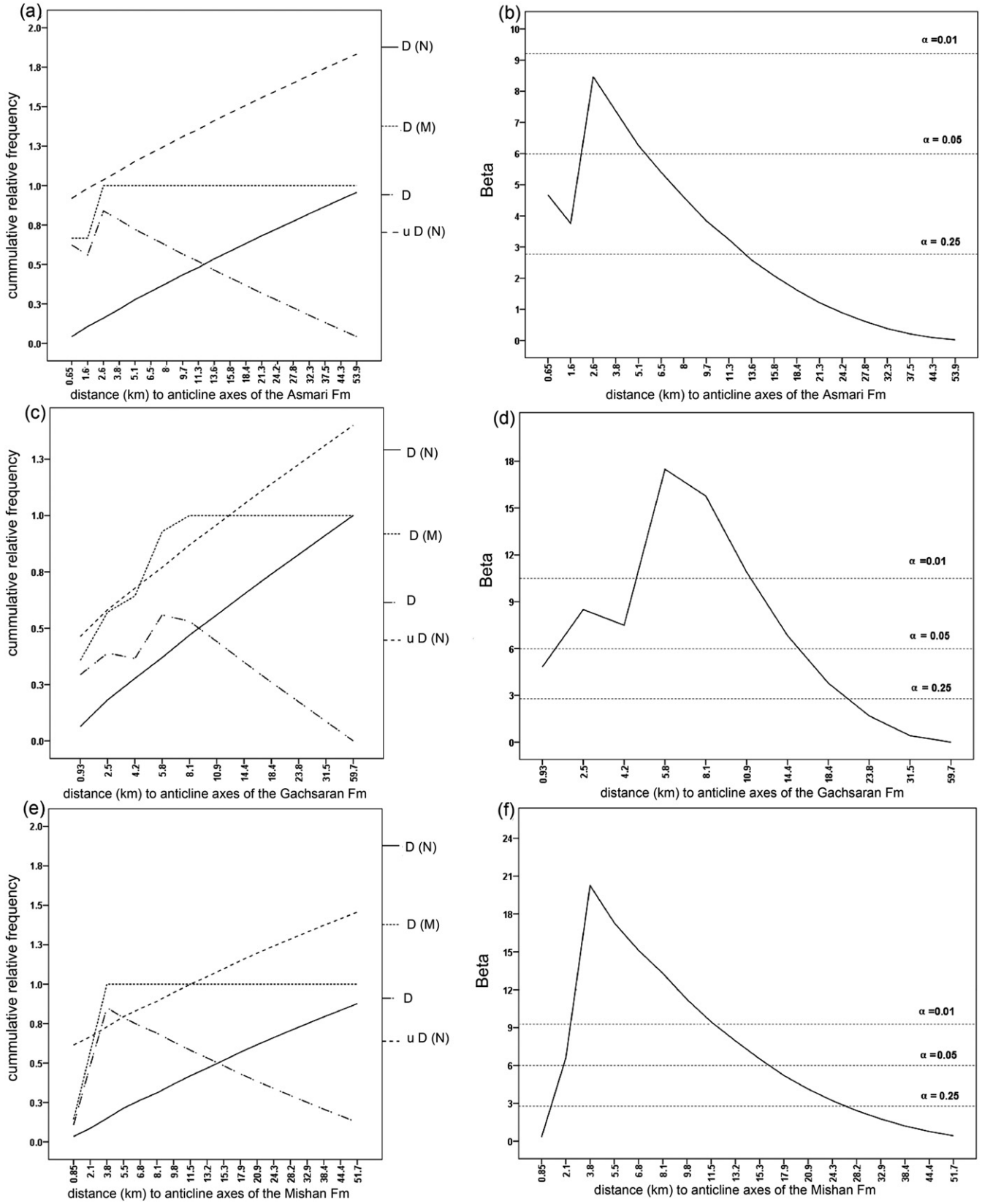

Figure 9. Graphs of cumulative relative frequency of distances at heavy oil or asphalt seep locations ($D(M)$) and non-heavy oil or asphalt locations ($D(N)$) around structural units of the three formations and corresponding graphs of β-statistics of differences (D) between the cumulative relative frequency curves, the Dezful Embayment. D and u $D(N)$ represent spatial association of seeps with structures and confidence band for $\alpha = 0.01$ respectively. (a) and (b) show the analysis of the spatial association between heavy oil or asphalt and anticline axis of the Asmari Formation; (c) and (d) represent the spatial association between heavy oil or asphalt and anticline axis of the Gachsaran Formation; (e) and (f) show the analysis of the spatial association of heavy oil or asphalt seeps with the Mishan Formation.

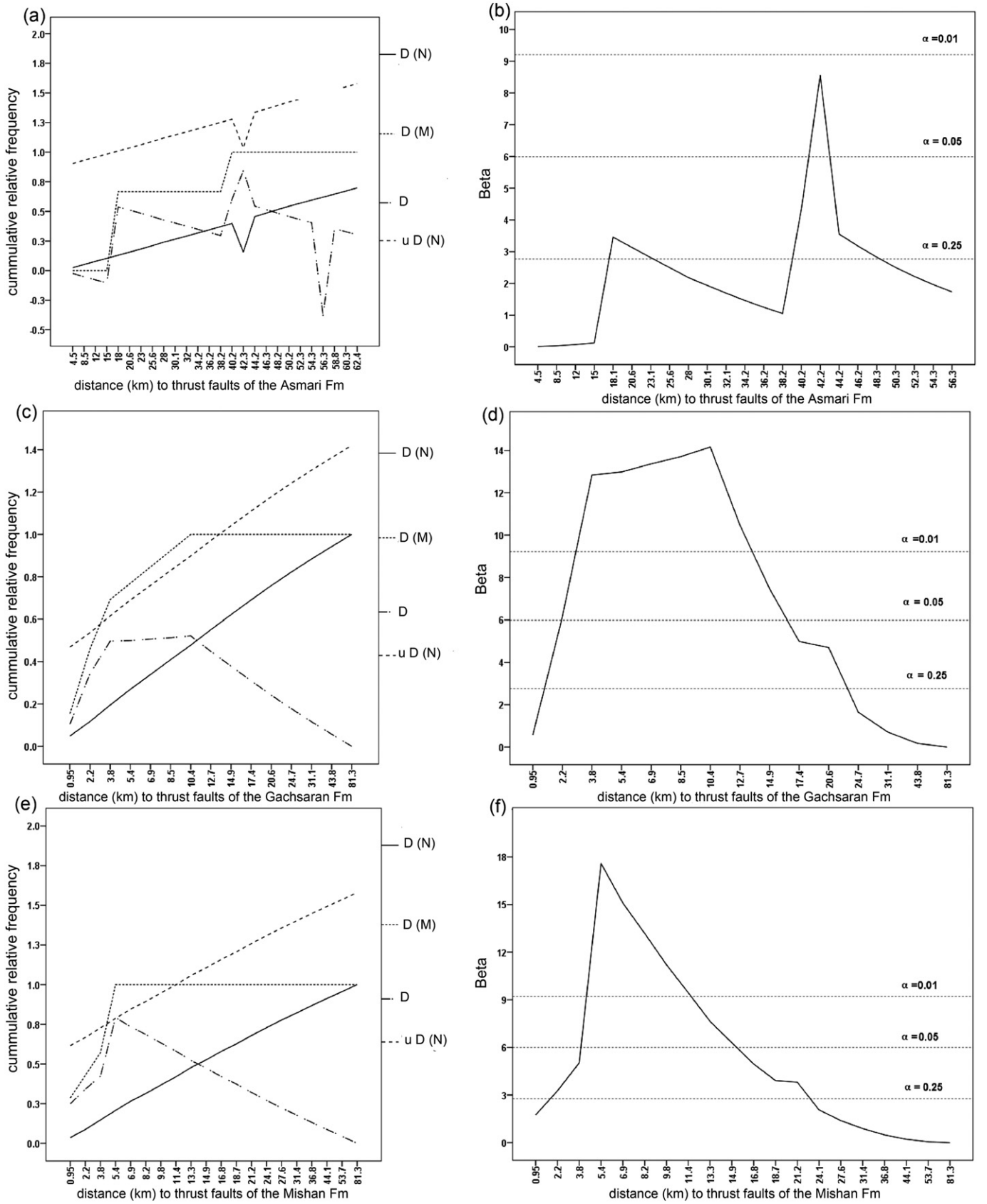

Figure 10. Graphs of cumulative relative frequency of distances at heavy oil or asphalt seep locations ($D(M)$) and non-heavy oil or asphalt locations ($D(N)$) around thrust faults of three formations and corresponding graphs of β-statistics of differences (D) between the cumulative relative frequency curves, the Dezful Embayment. D and u $D(N)$ represent spatial association of seeps with structures and confidence band for $\alpha = 0.01$ respectively. (a) and (b) show the analysis of spatial association between heavy oil or asphalt seeps and thrust faults of the Asmari Formation; (c) and (d) represent the spatial association between heavy oil or asphalt seeps and thrust faults of the Gachsaran Formation; and (e) and (f) show the spatial association between heavy oil or asphalt seeps and thrust faults of the Mishan Formation.

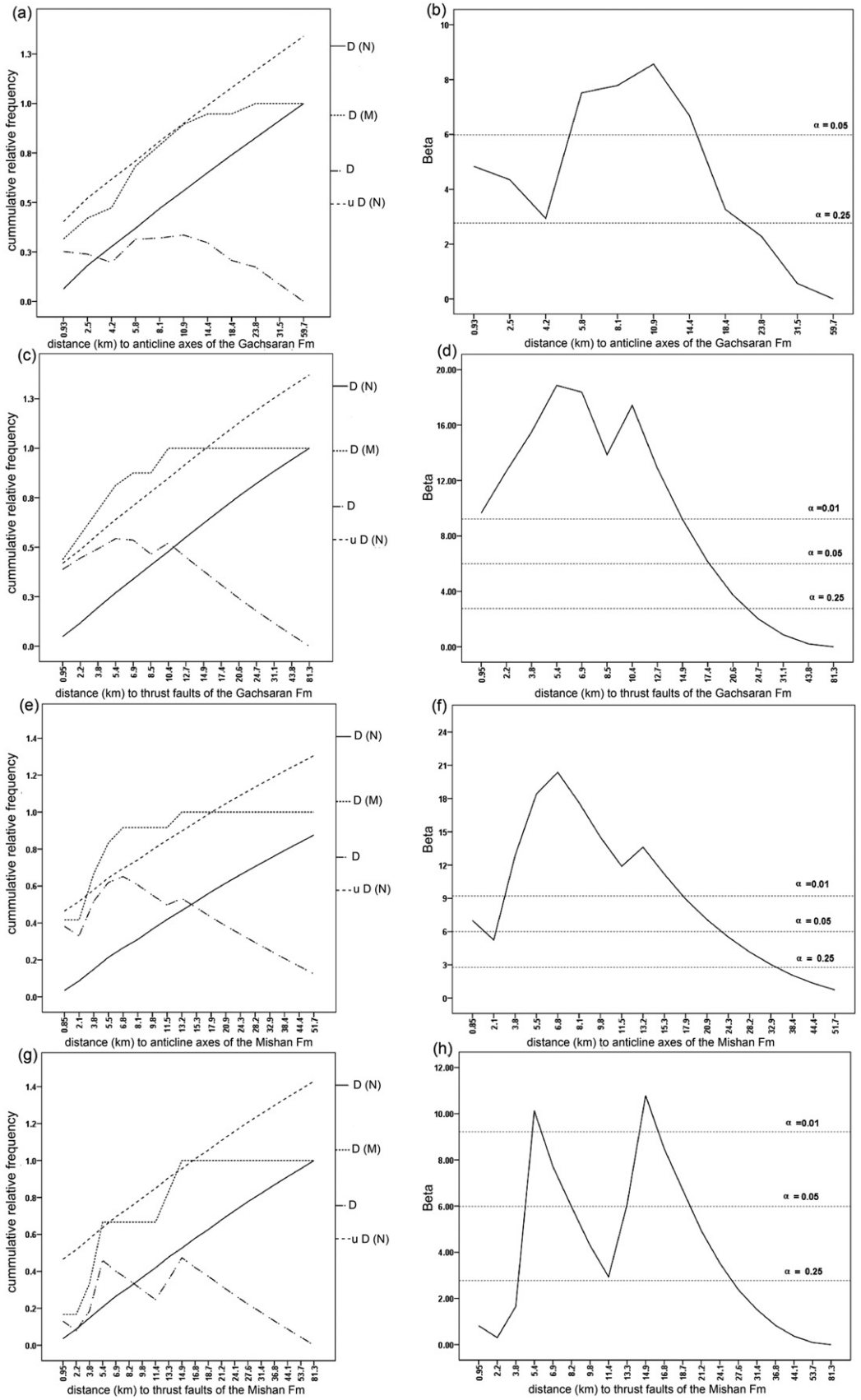

Figure 11. Graphs of cumulative relative frequency of distances at Gach-e-tursh locations ($D(M)$) and non-seep locations ($D(N)$) around structural units of the Gachsaran and Mishan formations and corresponding graphs of β-statistics of differences (D) between the cumulative relative frequency curves, the Dezful Embayment. D and u $D(N)$ represent spatial association of seeps with structures and confidence band for $\alpha = 0.01$ respectively. (a) and (b) show the analysis of spatial association between Gach-e-tursh and anticline axis of the Gachsaran Formation; (c) and (d) represent the spatial association between Gach-e-tusrh and thrust faults of the Gachsaran Formation; (e) and (f) show the analysis of spatial association between Gach-e-tursh and anticline axis of the Mishan Formation; and (g) and (h) show the analysis of spatial association between Gach-e-tursh and thrust faults of the Mishan Formation.

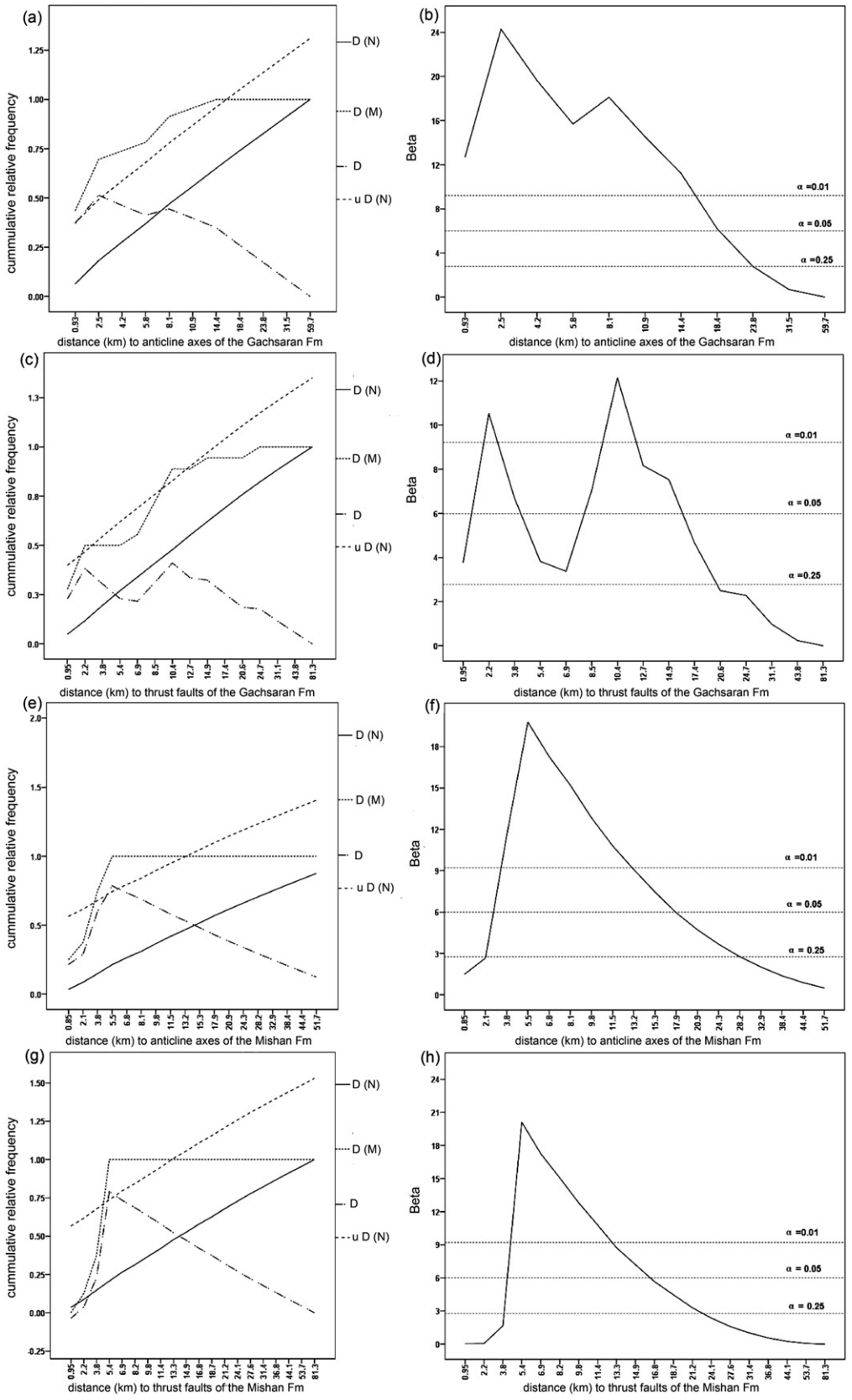

Figure 12. Graphs of cumulative relative frequency of distances at sulphur springs locations ($D(M)$) and non-seep locations ($D(N)$) around structural units of the Gachsaran and Mishan formations and corresponding graphs of β-statistics of differences (D) between the cumulative relative frequency curves, the Dezful Embayment. D and u $D(N)$ represent spatial association of seeps with structures and confidence band for $\alpha = 0.01$ respectively. (a) and (b) show the analysis of spatial association between sulphur springs and anticline axis of the Gachsaran Formation; (c) and (d) represent the spatial association between sulphur springs and thrust faults of the Gachsaran Formation; (e) and (f) show the analysis of spatial association between sulphur springs and anticline axis of the Mishan Formation; and (g) and (h) show the analysis of spatial association between sulphur springs and thrust faults of the Mishan Formation.

imply that there are two groups of sulphur springs in the area. The first group is comprised of about 50% of the sulphur springs located about an average of 2.2 km away from thrust faults of the Gachsaran. The second group is comprised of about 50% of springs located about an average of 10.4 km away from thrust faults in the Gachsaran Formation. In the Gachsaran Formation, the positive spatial association of sulphur springs with anticline axes is stronger than with thrust faults.

Sulphur springs show significant spatial associations (at $\alpha = 0.01$) with anticline axes and thrust faults in the Mishan Formation (Fig. 12e and g). These associations are optimal within 5.5 km of anticline axes and 5.4 km of thrust faults (Fig. 12f and h).

By means of spatial association analysis, it is possible to rank the individual sets of geological features in terms of their relative importance as controls on the occurrences of each sub-set of hydrocarbon seeps. In the distance distribution method, a basis for this ranking is the ratio of the value of $D(M)$ to the value of the $D(N)$ at the optimal distance of optimal positive spatial association of a set of geological feature (Carranza, 2009a). As summarized in Table 2, oil and gas seeps are mostly associated with the Mishan Formation and with structures in that formation. This finding suggests that hydrocarbons migrated upwards in the stratigraphy in the Dezful Embayment.

5. Conceptual modeling of occurrence of hydrocarbon seeps in the Dezful Embayment

The strong positive spatial associations of oil seeps and products of gas seeps alteration such as sulphur springs and Gach-e-tursh with the Mishan Formation and with anticline axes and thrust faults in that formation (Table 2) imply that densities of hydrocarbon seeps are not decreased upwards in the stratigraphy. The results of spatial association analyses (Figs. 9 and 10) imply that there are probably two groups of heavy oil or asphalt seeps. The first group is spatially associated with the Asmari anticlines exposed to the surface. The occurrence of this first group of seeps could be due to the final exhaustion of former oil accumulations in the Asmari reservoir. The second group is spatially associated with the Gachsaran cap rock and the overlying Mishan Formation, where heavy oil or asphalt seeps showed stronger positive spatial associations with structures in the Mishan Formation than in the Gachsaran cap rock (Table 2). Where the Gachsaran Formation is exposed to the surface and where it is overlain by the Mishan Formation, heavy oil or asphalt seeps show spatial associations with associated structures (Fig. 13a). Although the Gachsaran Formation has flowed by salt tectonics (Berberian, 1995), resulting in disharmonic relationship between folds in the surface and evaporites in the subsurface, oil likely escaped through prominent NW–SE and NE–SW trending faults and fractures formed during the Miocene syntectonic deposition of the Gachsaran Formation and/or through subsidiary N–S and NE–SW trending fractures formed by the reactivation of basement faults. In the former case, when oil migrated to pre-existing structures in the Asmari reservoir sealed by the Gachsaran cap rock in the late Miocene-Pliocene, hydrocarbons may have been localized in fractures related to salts and/or in NW–SE faults in SW flanks of anticlines. Later, localized hydrocarbons re-migrated upwards due to active tectonics in the area. The second case could have happened when N–S and NE–SW trending fractures formed by the shortening and the reactivation of basement faults breached the seal or superimposed the former structures.

When the Gachsaran Formation was buried (Fig. 13b), it likely acted as a detachment zone such that overlying formations may have been folded into anticlines. The axes of those anticlines were likely displaced to the SW with respect to fold crests within underlying strata (cf. Sherkati et al., 2005; Allen and Talebian, 2011). In this case, oil could have migrated through thrust faults in the southwestern flank of the Gachsaran cap rock and joined the NNE–SSW trending fault-related fractures. The oil could have lost its lighter components and occurred as heavy oil or asphalt seeps in the Mishan Formation at the surface. Hydrocarbon seeps could have occurred at the contact zone of the Mishan Formation with the Gachsaran cap rock. They likely found active faults related to salts of

Table 2
Summary of statistically significant results of analyses of spatial associations between each sub-set of hydrocarbon seeps and individual sets of structural features of the formations having positive spatial associations with seep. Values in bold represent statistically significant positive spatial associations.

Summary of statistically significant results of analyses of spatial associations between heavy oil or asphalt seeps and individual sets of structural features of three formations having positive spatial associations with seeps

Structural features	Distance (d) of optimal positive spatial association	Values of ($D(M)$) at d (see Figs. 6 and 7)	Values of $D(N)$ at d (see Figs. 6 and 7)	Values of ($D(M)$): $D(N)$ at d
Anticline axes of the Asmari Fm	2.6	100	0.16	6.2
Anticline axes of the Gachsaran Fm	5.8	0.93	0.37	2.5
Anticline axes of the Mishan Fm	3.8	1	0.14	**7.1**
Thrust faults of the Gachsaran Fm	10.4	1	0.48	2
Thrust faults of the Mishan Fm	5.4	1	0.2	5

Summary of statistically significant results of analyses of spatial associations between *Gach-e-tursh* and individual sets of structural features of tow Formations having positive spatial associations with seeps

Structural features	Distance (d) of optimal positive spatial association	Values of ($D(M)$) at d (see Fig. 8)	Values of $D(N)$ at d (see Fig. 8)	Values of ($D(M)$): $D(N)$ at d
Anticline axes of the Gachsaran Fm	10.9	0.89	0.55	1.6
Anticline axes of the Mishan Fm	6.8	0.91	0.26	**3.5**
Thrust faults of the Gachsaran Fm	5.4	0.81	0.26	3.1
Thrust faults of the Mishan Fm	14.9	1	0.52	1.9

Summary of statistically significant results of analyses of spatial associations between sulphur springs and individual sets of structural features of tow Formations having positive spatial associations with seeps

Structural features	Distance (d) of optimal positive spatial association	Values of ($D(M)$) at d (see Fig. 9)	Values of $D(N)$ at d (see Fig. 9)	Values of ($D(M)$): $D(N)$ at d
Anticline axes of the Gachsaran Fm	2.5	0.69	0.18	3.8
Anticline axes of the Mishan Fm	5.5	1	0.2	**5**
Thrust faults of the Gachsaran Fm	10.4	0.88	0.47	1.9
Thrust faults of the Mishan Fm	5.4	1	0.2	5

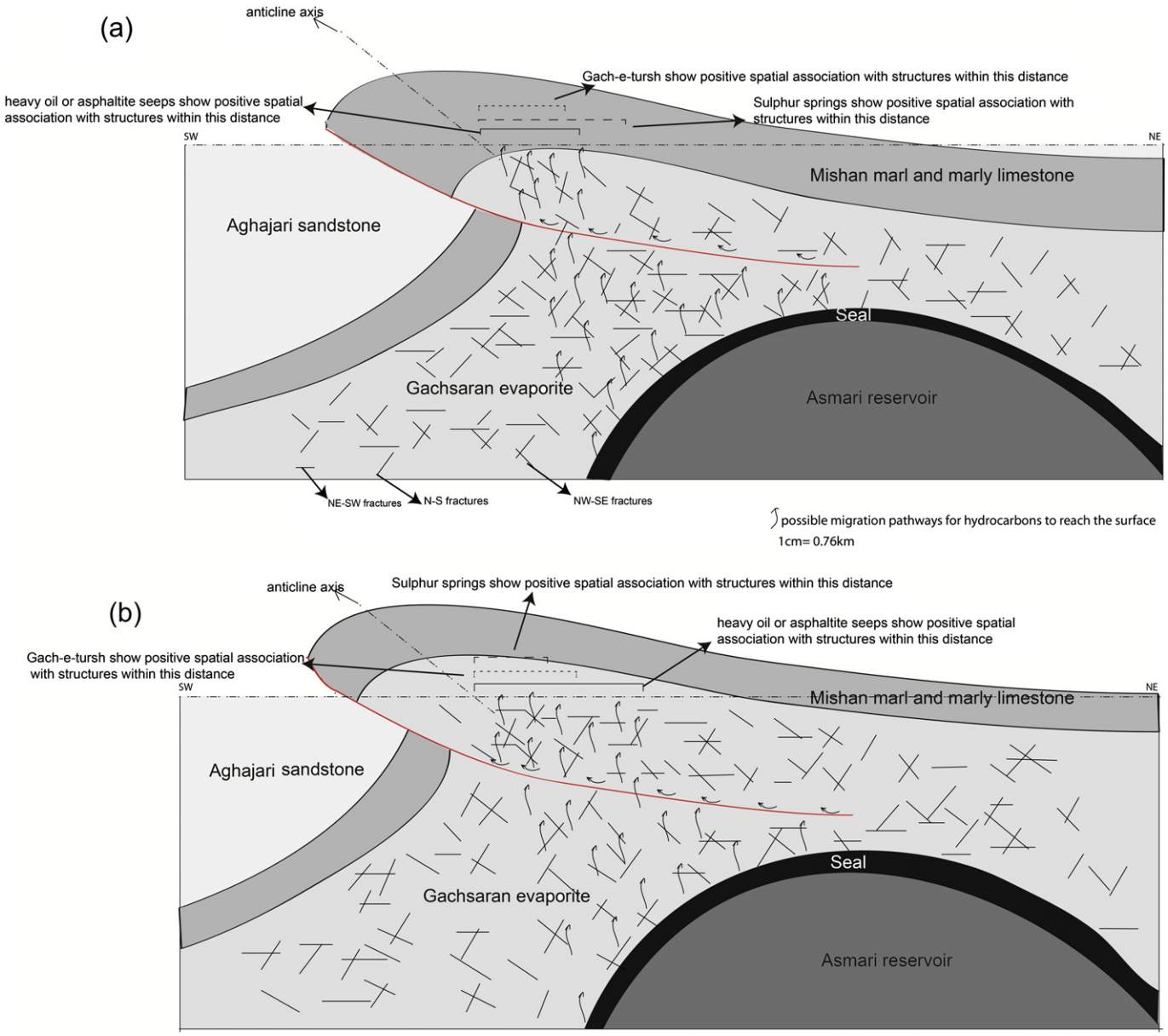

Figure 13. Conceptual model for the occurrence of onshore hydrocarbon seeps and their alteration products in the Dezful Embayment, (a) when the Gachsaran Formation has exposed at the surface and (b) when it is overlaid by the Mishan Formation.

the cap rock and a network of open fractures as migration pathways to reach the surface. Because the SW flanks of the Gachsaran anticlines are thrusted, heavy oil or asphalt seeps likely occurred at the southwestern parts of structures. In addition, the low permeability of marl of the Mishan Formation would have not allowed hydrocarbons to migrate to the surface through this Formation in the subsurface. The foregoing interpretations of results of the spatial analyses of heavy oil or asphalt seeps with structures and lithologic units suggest, therefore, that subsurface fractures and faults of the Gachsaran cap rock, particularly at the southwestern flank, provided favorable pathways for the vertical migration of these seeps to reach the surface.

The positive spatial associations of Gach-e-tursh and sulphur springs with the Gachsaran and Mishan structures (Figs. 11 and 12) imply that gas seeps have migrated upwards in stratigraphy and have produced these alterations in the respective formations. Gas-free oil seeps are rare or do not exist because oil buoyancy itself was not enough to reach the surface. However, gas may have segregated from oil in the subsurface and probably escaped through permeable fractures even when seal was effective and not breached by faults. Thus, gas may have probably migrated through NW–SE, and NNE–SSW trending fractures within the Gachsaran cap rock. Products of gas seep alteration such as Gach-e-tursh and sulphur springs have occurred within the Gachsaran Formation (Fig. 13a) or at the contact zone of the Gachsaran Formation with the Mishan Formation (Fig. 13b). The configuration of Gach-e-tursh at the surface as vein fillings or matrix cement could be an important factor for better understanding of gas seeps pathways mineralization. Gas may have entered basinal water and have changed its chemical properties. This water likely rose up and was enriched in sulphate by dissolution of anhydrite in the Gachsaran Formation. This action may have produced features such as galleries at the contact between limestone and gypsum following maximum dip in rhythmic units of the Gachsaran cap rocks in the subsurface and/or at the sharp

contact zone of the Gachsaran Formation with the Mishan Formation. Such features could have been potential conduits for fluid flow in the subsurface.

6. Discussion

The results of Fry analyses of hydrocarbon seep locations are useful for visual interpretations of which structures likely controlled the occurrence of hydrocarbon seeps in the Dezful Embayment. The syntheses of those results with the results of analyses of spatial association of seeps with geological features are useful for development of a conceptual model for the occurrence of onshore hydrocarbon seeps in the Dezful Embayment. In this conceptual model, we suggest that hydrocarbon seeps and their alteration products likely occur in the Mishan Formation. In areas where the Gachsaran cap rock does not outcrop, it is likely that hydrocarbon seeps and their alteration products occur on the surface of the overlying Mishan Formation. The deformation of the petroleum basin in the Dezful Embayment has resulted in faults and fractures, which were likely potential pathways for hydrocarbons to migrate upwards to the surface. The structural disharmony between the underlying carbonate reservoir and overlying folds, which resulted from salt tectonics, likely played a role in the lateral displacement of hydrocarbon seeps from their source rocks. However, oil cannot flow except under well conditions, governed by factors such as viscosity and capillarity. In some areas, oil was likely trapped at the water table where it had biodegraded or had flowed downward to emerge groundwater, although the associated gas could have escaped into the surface rocks.

Many oil fields in SW of Iran have a gas cap (Alshahran and Nairn, 1997); thus, a better understanding of the occurrences of gas seeps and their alteration products may benefit from petroleum-finding survey. However, an advantage of spatial analyses in the present study is the provision of empirical evidence for establishing a conceptual model of geological controls on hydrocarbon seep occurrence. Therefore, the methods of spatial analyses demonstrated here could provide geo-information that can be used as scientific basis for selecting potential areas for investigation of hydrocarbon entrapment.

Nevertheless, results of the application of the spatial analytical methods used in the present study can be undermined by the (lack of) quality and completeness of the datasets used and by the scale compatibility between the datasets. The datasets used here were derived from geological maps compiled by the Iranian oil company. Thus, the datasets used are compatible in scale although they may not be complete. Accordingly, there is a possibility that hydrocarbon seeps are associated with minor structures that were not mappable at the scale of map shown in Figures 3 and 4. It follows that the quantified spatial associations between hydrocarbons seeps and structures presented in this study are tentative. This means that the analyses and the conceptual model presented must be updated as new data become available.

7. Concluding remarks

With the aid of spatial pattern and spatial association analyses, a conceptual model for the occurrence of oil and gas seeps in the Dezful Embayment was developed. Oil seeps likely have migrated along NW–SE and NE–SW trending faults and fractures in SW flanks of anticlines, whereas gas seeps likely have escaped to the surface through prominent NW–SE and N–S trending faults and fractures. The positive spatial associations of seeps with the Mishan Formation imply that the density of seeps is not decreased upwards in the stratigraphy suggesting upward migration of hydrocarbons through permeable micro-fractures and micro-pores in their strata. Salt tectonics has played an important role in the lateral migration of hydrocarbon seeps from their sources.

Acknowledgment

The authors thank the European Union – in particular the Erasmus Mundus programmme – for financial support of the research.

References

Abdollahi Fard, M., Sepehr, M., sherkati, S., 2011. Neogene salt in SW Iran and its interaction with Zagros folding. Geological Magazin 148, 854–867.
Alavi, M., 2004. Regional stratigraphy of the Zagros fold-thrust belt of Iran and its proforland evolution. American Journal of Science 304 (January), 1–20.
Alshahran, A., Narin, A., 1997. Sedimentary Basins and Petroleum Geology of the Middle East. Elsevier Publishing.
Allen, M.B., Talebian, M., 2011. Structural variation along the Zagros and the nature of the Dezful Embayment. Geological Magazine 148, 911–924.
Bahroudi, A., Koyi, H.A., 2004. Tectono-sedimentary framework of the Gachsaran Formation in the Zagros foreland basin. Marine and Petroleum Geology 21 (10), 1295–1310.
Berberian, M., 1995. Master "blind" thrust faults hidden under the Zagros folds: active basement tectonics and surface morphotectonics. Tectonophysics 241 (3–4), 193–195.
Berberian, M., King, G.C.P., 1981. Towards a paleogeography and tectonic evolution of Iran. Cnadian Journal of Earth Sciences 18, 210–265.
Berman, M., 1977. Distance distributions associated with Poisson processes of geometric figures. Journal of Applied Probability 14, 195–199.
Beydoun, Z.R., Hughes, M.W., Stoneley, R., 1992. Petroleum in the Zagros Basin: a late Tertiary foreland basin overprinted onto the outer edge of the vast hydrocarbon-rich Paleozoic–Mesozoic passive margin shelf. In: Macqueen, R.W., Leckie, D.A. (Eds.), Foreland Basins and Fold Belts. AAPG Bulletin Memoir, vol. 55, pp. 307–336.
Bonham-Carter, G.F., 1994. Geographic Information Systems for Geoscientists: Modelling with GIS. In: Computer Methods in the Geosciences, vol. 13. Pergamon Press, Oxford, U.K. p. 398.
Bordenave, M.L., 2002. The Middle Cretaceous to Early Miocene Petroleum System in the Zagros Domain of Iran, and Its Prospect Evaluation. AAPG Annual Meeting, Houston, Texas, March, pp. 10–13.
Bordenave, M.L., Hegre, J.A., 2005. The influence of tectonics on the entrapment of oil in the Dezful Embayment, Zagros foldbelt, Iran. Journal of Petroleum Geology 28 (4), 339–368.
Bordenave, M.L., Hegre, J.A., 2010. Current distribution of oil and gas field in the Zagros fold belt of Iran and contiguous offshore as the result of the petroleum systems. Geological Society of London 330, 291–353.
Carranza, E.J.M., 2009a. Controls on mineral deposit occurrence inferred from analysis of their spatial pattern and spatial association with geological features. Ore Geology Reviews 35 (3–4), 383–400.
Carranza, E.J.M., 2009b. In: Hale, M. (Ed.), Geochemical Anomaly and Mineral Prospectivity Mapping in GIS. Handbook of Exploration and Environmental Geochemistry, vol. 11. Elsevier B.V..
Carranza, E.J.M., Sadeghi, M., 2010. Predictive mapping of prospectivity and quantitative estimation of undiscovered VMS deposits in Skellefte district (Sweden). Ore Geology Reviews 38 (3), 219–241.
Carruba, S., Cesare, R.P., Buonaguro, R., Calabro, R., Carpi, R., Naini, M., 2006. Structural Pattern of the Zagros Fold-and-thrust Belt in the Dezful Embayment (SW Iran). Geological society of America. pp. 11–32.
Clarke, R.H., Cleverly, R.W., 1991. petroleum seepage and post-accumulation migration. In: England, W.A., Fleet, A.J. (Eds.), Petroleum Migration. Geological Society of London, Special Publication No.59, pp. 265–271.
De Boever, E., Huysmans, M., Muchez, P., Dimitrov, L., Swennen, R., 2009. Controlling factors on the morphology and spatial distribution of methane-related tubular concretions – case study of an Early Eocene seep system. Marine and Petroleum Geology 26 (8), 1580–1591.
Ding, F., Spiess, V., Brüning, M., Fekete, N., Keil, H., Bohrmann, G., 2008. A conceptual model for hydrocarbon accumulation and seepage processes around Chapopote asphalt site, southern Gulf of Mexico: from high resolution seismic point of view. Journal of Geophisical Research 113.
Douglas Elmore, R., Farrand, W.R., 1981. Asphalt-bearing sediment in Synorogenic Miocene-Pliocene Molasse, Zagros Mountain, Iran. AAPG Bulletien.
Edgell, H., 1996. Salt tectonism in the Persian Gulf basin. In: Alsop, G.I., Blundell, D.J., Davison, I. (Eds.), Salt Tectonics. Geological Society, London, Special Publications, vol. 100, pp. 129–151.
Ellis, J.M., Davis, H.H., Zamudio, J.A., Sept 2001. Exploring for onshore oil seeps with hyperspectral imaging. Oil and Gas Journal 10, 49–56.
Etiope, G., Papatheodorou, G., Christodoulou, D., Ferentinos, G., Sokos, E., Favali, P., 2006. Methane and hydrogen sulfide seepage in the NW Peloponnesus petroliferous basin (Greece): origin and geohazard. AAPG Bulletien 90 (5), 701–713.
Falcon, N.L., 1974. Southern Iran: Zagros mountains. In: Spencer, A. (Ed.), Mesozoic–Cenozoic Orogenic Belts. Geological Society of London, Special Publication, vol. 4, pp. 199–211.

Fry, N., 1979. Random point distributions and strain measurement in rocks. Tectonophysics 60, 89–105.
Gill, W.D., Ala, M.A., 1972. Sedimentology of Gachsaran formation (Lower Fars Series), southwest Iran. AAPG Bulletin 56, 1965–1974.
Hessami, K., Koyi, H.A., Talbot, C.J., 2001. The significance of strike-slip faulting in the basement of the Zagros fold and thrust belt. Journal of Petroleum Geology 24 (1), 5–28.
Huang, B., Xiao, X., Li, X., Cai, D., 2009. Spatial distribution and geochemistry of the nearshore gas seepages and their implications to natural gas migration in the Yinggehai Basin, offshore South China Sea. Marine and Petroleum Geology 26 (6), 928–935.
James, G.A., Wynd, J.G., 1965. Stratigraphic nomenclature of Iranian oil consortium agreement area. AAPG Bulletin 49, 2182–2245.
Jin, Y.K., Kim, Y.-G., Baranov, B., Shoji, H., Obzhirov, A., 2011. Distribution and expression of gas seeps in a gas hydrate province of the northeastern Sakhalin continental slope, Sea of Okhotsk. Marine and Petroleum Geology 28 (10), 1844–1855.
Kashfi, M., 1980. Stratigraphy and environmental sedimentology of lower Pars group (Miocene), south-southwest Iran. The American Association of Petroleum Geologists 64, 2095–2107.
Lacombe, O., Bellahsen, N., Mouthereau, F., 2011. Fracture patterns in the Zagros simply folded belt (Fars, Iran): constraints on early collisional tectonic history and role of basement faults. Geological Magazin, 1–24.
Leifer, I., Boles, J., 2005. Measurement of marine hydrocarbon seep flow through fractured rock and unconsolidated sediment. Marine and Petroleum Geology 22 (4), 551–568.
Leifer, I., Boles, J., 2006. Corrigendum to: measurement of marine hydrocarbon seep flow through fractured rock and unconsolidated sediment: [Marine and Petroleum Geology 22 (2005), 551–558]. Marine and Petroleum Geology 23 (3), 401.
Link, W.K., 1952. Significance of oil and gas seeps in world oil exploration. AAPG Bulletin 36, 1505–1541.
MacGregor, D.S., 1993. Relationships between seepage, tectonics and subsurface petroleum reserves. Marine and Petroleum Geology 10 (6), 606–619.
McQuillan, H., 1991. The role of basement tectonics in the control of sedimentary facies, structural patterns and salt plug emplacements in the Zagros fold belt of southwest Iran. Journal of Southeast Asian Earth Sciences 5 (1–4), 453–463.
Mobasher, K., Babaie, H., 2007. Kinematic significance of fold- and fault-related fracture systems in the Zagros mountains, southern Iran. Tectonophysics 451, 156–169.
Motiei, H., 1993. Stratigraphy of Zagros. Geological Survey of Iran (in Farsi). p. 536.
O'Berian, C.A.E., 1957. Salt diapirism in south Persia. Geologie en Mijnbouw 19, 357–376.
O'Brien, G.W., Lawrence, G.M., Williams, A.K., Glenn, K., Barrett, A.G., Lech, M., Edwards, D.S., Cowley, R., Boreham, C.J., Summons, R.E., 2005. Yampi Shelf, Browse Basin, North-West Shelf, Australia: a test-bed for constraining hydrocarbon migration and seepage rates using combinations of 2D and 3D seismic data and multiple, independent remote sensing technologies. Marine and Petroleum Geology 22 (4), 517–549.
Pinet, N., Duchesne, M., Lavoie, D., Bolduc, A., Long, B., 2008. Surface and subsurface signatures of gas seepage in the St. Lawrence Estuary (Canada): significance to hydrocarbon exploration. Marine and Petroleum Geology 25 (3), 271–288.
Rudkiewicz, J.L., Sherkati, S., Letouzey, J., 2007. Evolution of maturity in Northern Fars and in the Izeh zone (Iranian Zagros) and link with hydrocarbon prospectivity. In: Lacombe, O., Roure, F., Lavé, J., Vergés, J. (Eds.), Thrust Belts and Foreland Basins. Springer Berlin Heidelberg, pp. 229–246.
Safari, H.O., Pirasteh, S., Mansor, S.B., 2011. Role of the Kazerun fault for localizing oil seepage in the Zagros Mountain, Iran: an application of GiT. International Journal of Remote Sensing 32 (1), 1–16.
Sella, G.F., Dixon, T.H., Mao, A., 2002. A model for recent plate velocities from space geodesy. Journal of Geophisical Research 107, 11.11–11.30.
Sepehr, M., Cosgrove, J.W., 2002. The Major Fault Zones Controlling the Sedimentation, Deformation and Entrapment of Hydrocarbon in the Zagros Fold-thrust Belt, Iran: AAPG Annual Meeting, Houston, Texas, March 10–13.
Sherkati, S., Letouzey, J., 2004. Variation of structural style and basin evolution in the central Zagros (Izeh zone and Dezful Embayment), Iran. Marine and Petroleum Geology 21 (5), 535–554.
Sherkati, S., Molinaro, M., De Lamotte, D.F., Letouzey, J., 2005. Detachment folding in the central and eastern Zagros fold belt (Iran): salt mobility, multiple detachment and late basement control. Journal of Structural Geology 27 (9), 1680–1690.
Stephenson, B.J., Koopman, A., Hillgratner, H., Mc Quillan, H., Bourne, S., Noad, J.J., Rawnsley, K., 2007. Structural and stratigraphic controls on fold related fracturing in the Zagros mountains, Iran: implications for reservoir development. From. In: Lonergan, L., Jolly, R.J.H., Rawnsley, K., Sanderson, D.J. (Eds.), Fractured Reservoirs. Geological Society, London, Special Publications, vol. 270, pp. 1–21.
Stocklin, J., 1968. Structural history and tectonics of Iran. A review. AAPG Bulletin 52, 1229–1258.
Thomas, A.N., 1952. "Gach-i-turush" and associated phenomena in southwest Persia. V11 Convegno Nazionale Del Metano E Del Petrolio Taormina, section 1, preprint.
Warren, J.,K., 2006. Evaporites. Springer, Germany.
Washburn, L., Clark, J.F., Kyriakidis, P., 2005. The spatial scales, distribution, and intensity of natural marine hydrocarbon seeps near Coal Oil Point, California. Marine and Petroleum Geology 22 (4), 569–578.
Wennberg, O.P., Azizzadeh, M., Aqrawi, A.A.M., Blanc, E., Brockbank, P., Lyslo, K.B., Pickard, N., Salem, L.D., Svana, T., 2007. The Khaviz anticline: an outcrop analogue to giant fractured Asmari Formation reservoirs in SW Iran. From. In: Lonergan, L., Jolly, R.J.H., Rawnsley, K., Sanderson, D.J. (Eds.), Fractured Reservoirs. Geological Society, London, Special Publications, vol. 270, pp. 23–42.